Abstract

Thermally induced fractures or thermal cracks, and pronounced seismic events as snowquakes were studied at Mizuho Station, East Antarctica from June 1976 to January 1977. Fractures due to thermal stress were found in the uppermost 50 cm of the snow cover as a result of snow temperature decrease at the surface, and fracture under tensile thermal stress occurs when the stress exceeds the tensile strength of snow. Once thermal cracks are initiated, stress concentration occurs at tips of cracks, and fractures occur more easily in the smaller thermal stress than the tensile strength of snow and accompany more easily pronounced seismic events, that is, snowquake.

Snowquakes occur during the decrease of temperature and then thermally induced strain rate corresponds to ductile fracture of snow. The individual snowquakes occur in the near surface and the epicenters of snowquakes located by seismic observations are found near thermal cracks, which indicates that snowquake is caused by the formation of cracks. The epicenters are not distributed in a well-ordered sequence, thus the fractures of snow cover occur at random in the near surface which is under the tensile stress during the decrease of snow temperature.

1. Introduction

Many thermal cracks exist on the glazed surface in the Antarctic ice sheet and pronounced seismic events as the so-called ice shocks with loud sound have been experienced very often during the winter season. Thermal cracks are usually found on the glazed surface which is distributed in the region where katabatic wind prevails and the glazed surface is related closely to the absence of snow accumulation or long-term hiatus in snow stratigraphy (WATANABE, 1978). SWITHINBANK (1957) remarks that narrow cracks in the surface snow of the Maudheim Ice Shelf are observed only during winter and suggests that they have resulted from thermal contraction. However, physical processes of formation of thermal cracks are not studied well in terms of the initiation of thermal cracks and the mechanical properties of snow. It is, therefore, very important to reveal characteristics of thermal cracks and their behavior.

OMOTE *et al.* (1955) and HAMAGUCHI *et al.* (1977) studied the fracture of ice plate of the Lake Suwa in central Japan. They considered that the phenomenon of ice shock might represent a model of seismic source and the plate tectonic theory, because the ice plate and the water beneath it give a good model for lithosphere and asthenosphere of the earth. The ice faulting corresponds to the cataclysmic event due to the interaction of plate motions which is thought to be the main cause of geophysical and geological processes of the earth's crust. NEAVE and SAVAGE (1970) observed swarms of icequakes which occurred in the Athabasca Glacier (52.2°N, 117.2°W) to test a hypothesis that deep-focus earthquakes were caused by creep-instability mechanisms. They concluded that all the events appeared to be originated from extensional faulting near the surface of the glacier and most of the icequakes occurred within the zone of marginal crevasses. The individual events in an icequake swarm were distributed along a straight line of visible crevasse. Recently, KAMINUMA and TAKAHASHI (1975) observed snowquakes with one vertical seismograph at Mizuho Station for a short period in 1973, aiming at finding the characteristics of earthquake through the phenomenon of snowquake activity. They found that the prolonged low temperatures at night, especially when the air temperature drops below $-35°C$, caused pronounced seismic events as the results of snow contraction.

Although these authors have studied ice shocks or snowquakes, there is no precise interpretation on the mechanism of ice shock or snowquake because of the lack of proper understanding of physical properties of the medium such as the ice plate or the snow cover. Giving an emphasis on the physical properties of polar snow and the physical processes of snow fracture, the present author investigated the thermally

induced fractures and snowquake activities of polar snow cover at Mizuho Station, East Antarctica, in 1976. In this paper, the snowquake is defined as the fracture of snow, whereas icequake is the fracture of ice. The present paper deals with four aspects, *i.e.*, the formation of thermal cracks and snowquakes in association with characters of the snow temperature profiles, distribution of the glazed surface and variation of width of thermal crack, snowquake activities and mechanical properties of the snow cover in relation to thermally induced fractures.

2. Observation Site and Measurements

From June 1976 to January 1977, the present author observed snow temperature profiles, change of widths of thermal cracks and snowquake activities by means of seismographs at Mizuho Station. The station is located at 70°42′S and 44°20′E about 280 km southeast of Syowa Station, 2230 m in elevation, 2100 m in ice thickness and the annual mean air temperature of about −33°C (Fig. 1). The observational area (about 200×200 m) is in the lee of prevailing wind about 100 m east of Mizuho Station (Fig. 2). The observation sites for the width of thermal cracks, a seismograph tripartite (vertical component) and the thermal crack observation area were set in the observational area. A large glazed surface area surrounds Mizuho Station and the glazed surface sometimes lacks annual layers. The surface snow density is 0.35 to 0.45 g/cm^3 (WATANABE and YOSHIMURA, 1972).

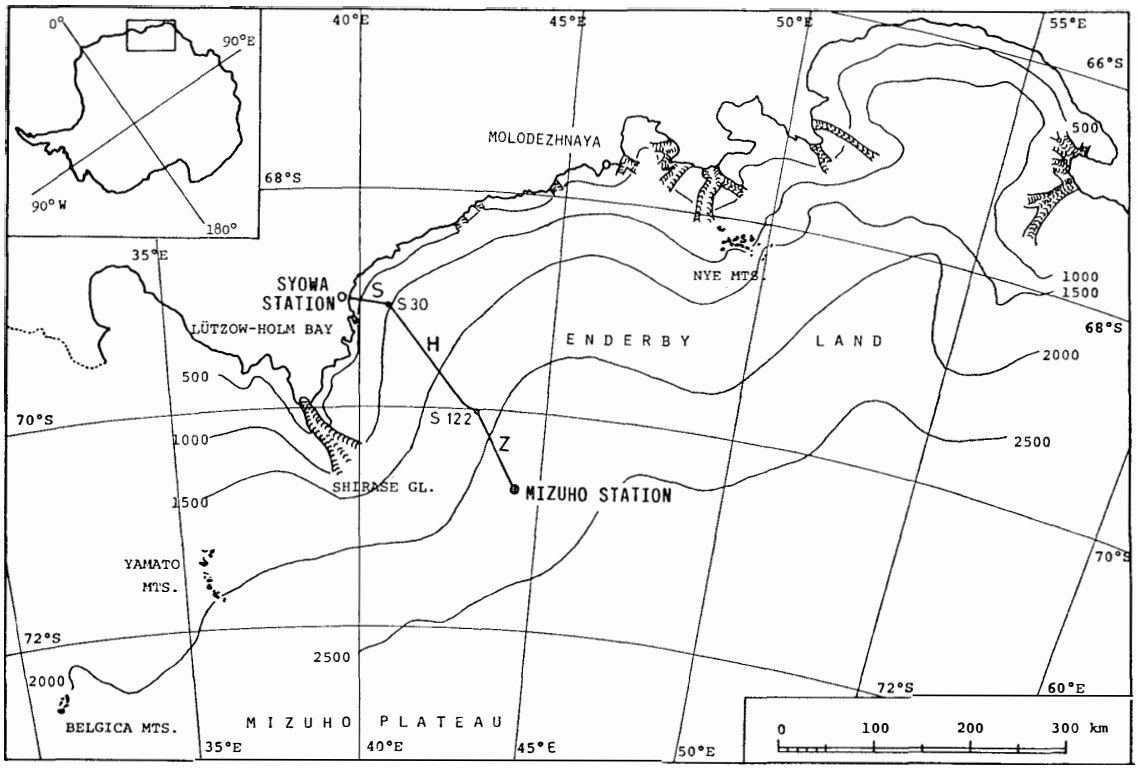

Fig. 1. Location of Mizuho Station (70°41′53″S, 44°19′54″E; 2230 m above sea level; ice thickness 2100 m).

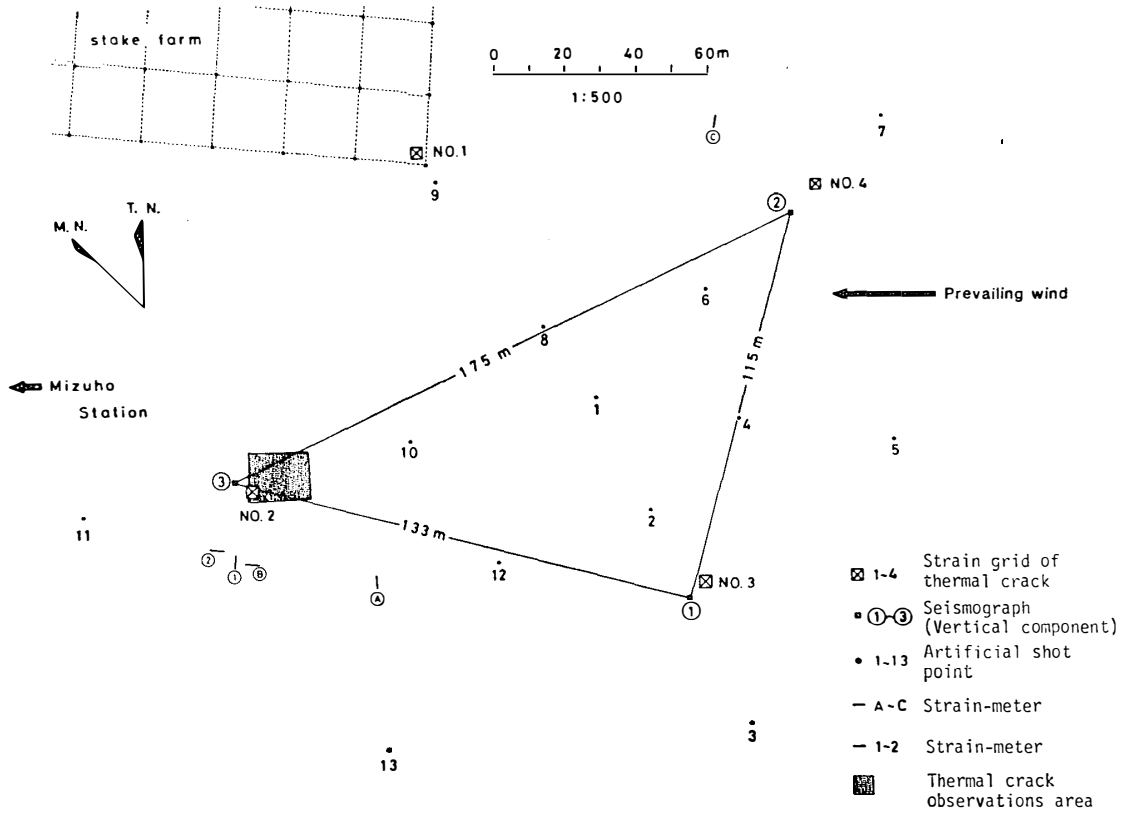

Fig. 2. Sketch map of observation site for the width of thermal cracks (Nos. 1–4), a seismograph tripartite and the thermal crack observation area.

2.1. Snow temperature profiles

Ten thermistors were buried in the snow near No. 3 seismograph shown in Fig. 2 and continuous records were obtained from May 26, 1976 to January 25,1977. Thermistors were set at the surface (about 1 cm deep), and at depths of 0.1, 0.2, 0.3, 0.5, 1, 2, 3, 5 and 10 m; sensors in the upper levels were covered with white stainless steel tube to reduce radiation errors. The output of thermistors was continuously recorded by a 12-channel recorder and the overall accuracy of the measurements was ± 0.3°C. In the present paper, the snow surface temperature is defined as the snow temperature measured at a depth of about 1 cm.

2.2. Width of thermal cracks

Many glazed surface areas were found on the snow surface around Mizuho Station, and most of the thermal cracks were developed on the glazed surface. The observation area of thermal cracks, which is shown with a hatched area in Fig. 2, was kept intact and the observation of patterns of thermal cracks has been carried out since July 1970 (WATANABE and YOSHIMURA, 1972).

To investigate the formation of thermal cracks and the opening and closing of thermal cracks, widths of thermal cracks were measured once a day at four sites, where three of them (Nos. 2, 3 and 4) were located near the seismographs and No. 1 was installed in the stake farm as shown in Fig. 2. The distance of two reference points across a crack was measured with a vernier calliper with the accuracy of measurements to the nearest 1/20 mm (Fig. 3a). The reference points were made of stainless steel

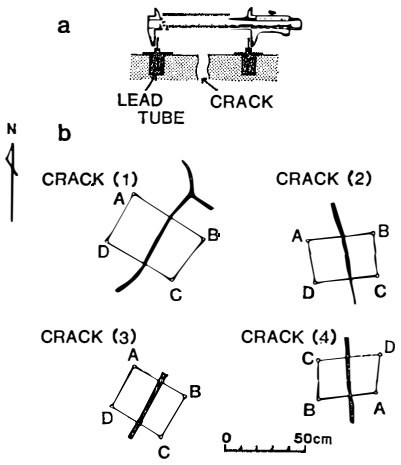

Fig. 3. Method of measurement of distance between two reference points across a thermal crack (a); and configuration of four grids composed of four reference points (b).

tube which was tightly inserted into the holes in the surface snow layer. As illustrated in Fig. 3b four reference points of A, B, C and D were prepared to form a square with sides of about 40–50 cm across thermal crack at four sites (Nos. 1, 2, 3 and 4) as shown in Fig. 2. The distances between four reference points such as the sides of $\overline{AB}$, $\overline{BC}$, $\overline{CD}$, $\overline{DA}$, $\overline{AC}$ and $\overline{BD}$ were measured by the vernier calliper and the reading of vernier calliper was corrected for the air temperature, that is, the corrected value of distance between two reference points was obtained, subtracting an appropriate temperature correction at 0°C from the readings of the distance.

2.3. Snowquake activities

Three electromagnetic seismographs (vertical component) of moving-coil type were used to detect elastic waves of snowquakes. As illustrated in Fig. 4, the frequency response of seismograph with the natural frequency of 1 Hz was measured on the shaking table, giving flat characteristics in the frequency range of 1–50 Hz. The seismographs were installed in a snow pit at a depth of about 50 cm to reduce wind-generated noise; they were in the distance of about 200 m to the east from the facilities of Mizuho Station where artificial ground noises, such as the noise of power supply generator, originate. Hence, all the recording of seismographs installed in the snow pit was done to take advantage of the lower noise level. To determine the epicenters of snowquakes near the snow surface, the seismographs were arrayed in a triangle (tripartite) with the sides of 115, 175 and 133 m. Seismograph signals were transmitted with cables and recorded at Mizuho Station. The signals were fed to an amplifier

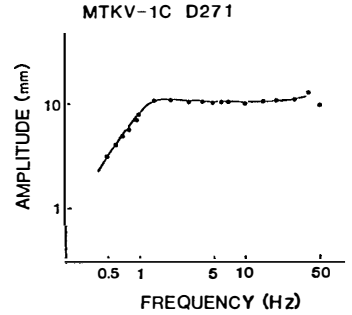

Fig. 4. Frequency response of seismograph (natural frequency 1 Hz) measured on the shaking table, in which the response is uniform in the frequency range of 1–50 Hz.

and recorded on a portable data-recorder (TEAC, R70A) with a cassette tape at a speed of 4.76 cm/s. Playback of the cassette tape was carried out with a four-channel precision tape recorder (Model SDR-803, Hikari Tsushinki Co., Ltd.). The playback speed was 1/20th of the recording speed, using a four-penrecorder with a 0.9 Hz high pass filter. The normalized overall frequency response of the recording and playback system is shown in Fig. 5, which indicates the flat frequency response in the range of more than 50 Hz.

Figure 6 shows an example of snowquake signals recorded with the tripartite. Since three seismograph outputs and 1-second time mark from a chronometer were recorded simultaneously on the same tape, arrival time differences between seismographs were measured precisely. The chronometer calibration was made with the time signal of JJY at 12-hour to 6-day intervals. The 1-second time marks were used for correcting the very minor fluctuation in the paper speed of the penrecorder, which gave a negligible correction.

The observation of snowquake activities with the seismographs and the recording system was carried out between June 1976 and January 1977. No natural earthquakes were detected during this period, but very many swarm type snowquakes were recorded.

To determine the propagation velocity of longitudinal waves (V_p) in snow around Mizuho Station, the refraction shooting method was used to calculate V_p from the travel-time curve as shown in Fig. 7. Three seismographs were spaced at 20 m intervals

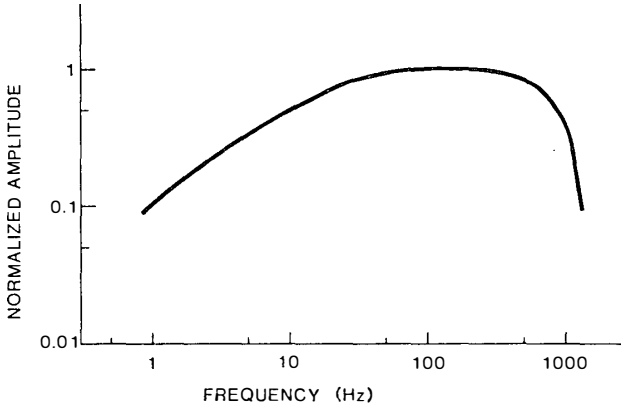

Fig. 5. Normalized overall frequency response of the recording and playback system.

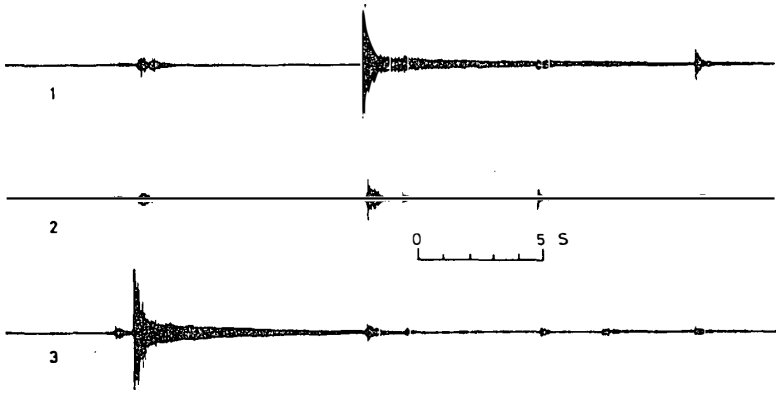

Fig. 6. A record of snowquake signals from the three seismograph array. Numerals correspond to the signals from seismograph Nos. 1, 2 and 3.

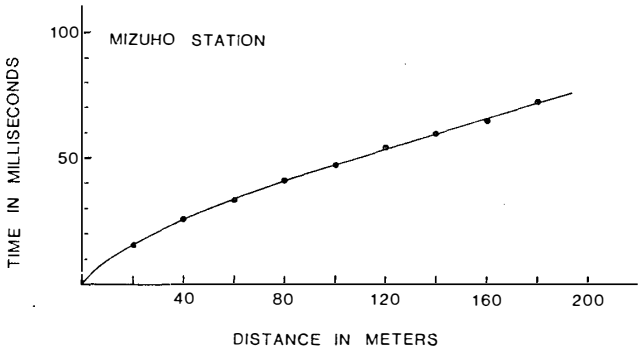

Fig. 7. Travel-time curve for refraction at Mizuho Station.

and elastic waves at the snow surface were generated by the artificial shot with a steel hammer at distances up to 200 m to the east from the end of the seismograph line near the seismograph site No. 3 in Fig. 2. Therefore, the velocity profile of longitudinal waves in the snow cover was determined from the travel-time curve.

On the other hand, snow density of core samples at Mizuho Station was measured in detail by NARITA *et al.* (1978). The overall density-depth curve shows that near the snow surface the mean density is around 0.40 g/cm^3 and increases with the depth, and it reaches 0.84 g/cm^3 at about 55 m. Taking this density profile into consideration, ISHIZAWA (1981) discussed the velocity profile of longitudinal wave down to 80 m at Mizuho Station where he carried out wave velocity observations in 1978.

The travel-time curve obtained by the refraction shooting method was used to determine the location of each snowquake epicenter by an iterative least-square procedure from the arrival times of longitudinal waves. At first, an appropriate position of snowquake epicenter was assumed as the initial location; then the travel-time curve

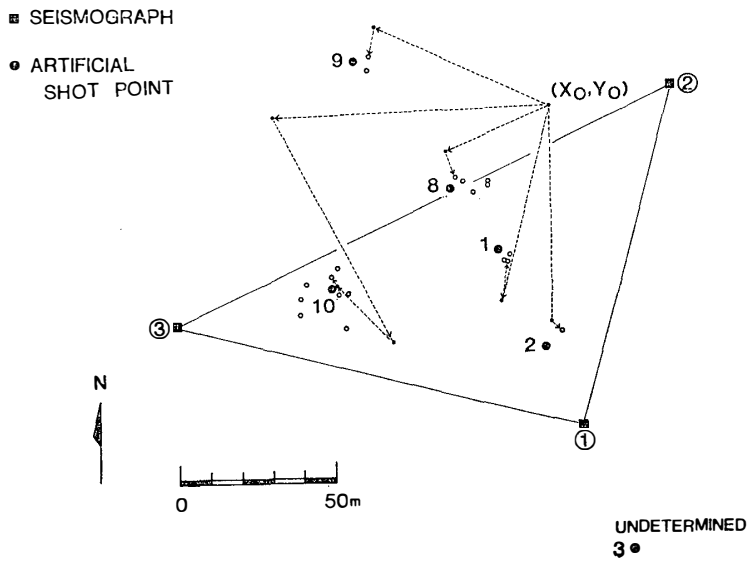

Fig. 8. Calculated positions (white circles) of artificial shots by means of an iterative least-square procedure from arrival times of P waves at each seismograph and positions of the artificial shots (black dots). Coordinates (X_0, Y_0) indicate the initial location to start the iterative least-square procedure to determine the calculated positions; arrows with dotted line indicate the features of converging to the calculated positions.

between the assumed location and each seismograph site is calculated from the travel-time curve measured by the refraction shooting method, and the least-square procedure was iterated to determine the accurate snowquake epicenter. The accuracy of this procedure was estimated by comparing the calculated position of artificial shots from the arrival times of longitudinal waves detected at each seismograph with the actual position of artificial shots. In Fig. 8, six artificial shots (1, 2, 3, 8, 9 and 10) on the snow surface are shown and these positions are directly measured with reference to the seismograph sites. The artificial shots were also used to check for polarity reversals both in recording and playback system. In general, the accuracy of position determined by means of the tripartite method is usually good within the array, but the accuracy deteriorates outside the array. As illustrated in Fig. 8, the calculated positions of artificial shots within the array are within about ± 10 m, including shot site 9 outside the array, though at shot site 10 the error is in the order of ± 20 m. At shot site 3 outside the array, the calculated position was not obtained by means of an iterative least-square procedure, because the signals recorded at seismograph No. 3 were very weak. Thus, it is considered that the position of snowquake epicenter within the array is determined with an accuracy of the order of ± 10 m.

3. Temperature Variations in the Surface Snow Cover

The snowquakes around Mizuho Station occurred when the air temperature decreased (KAMINUMA and TAKAHASHI, 1975), consequently crackes in the surface snow layer were formed, namely thermal cracks. Since the snowquake activities are closely associated with the variations of snow temperature near the surface snow layer, temperature regime will be examined.

Figure 9 shows the mean daily snow temperature at the surface, and at depths of 0.1, 0.2, 0.3, 0.5, 1, 2, 3, 5 and 10 m for the period from June 1976 to January 1978.

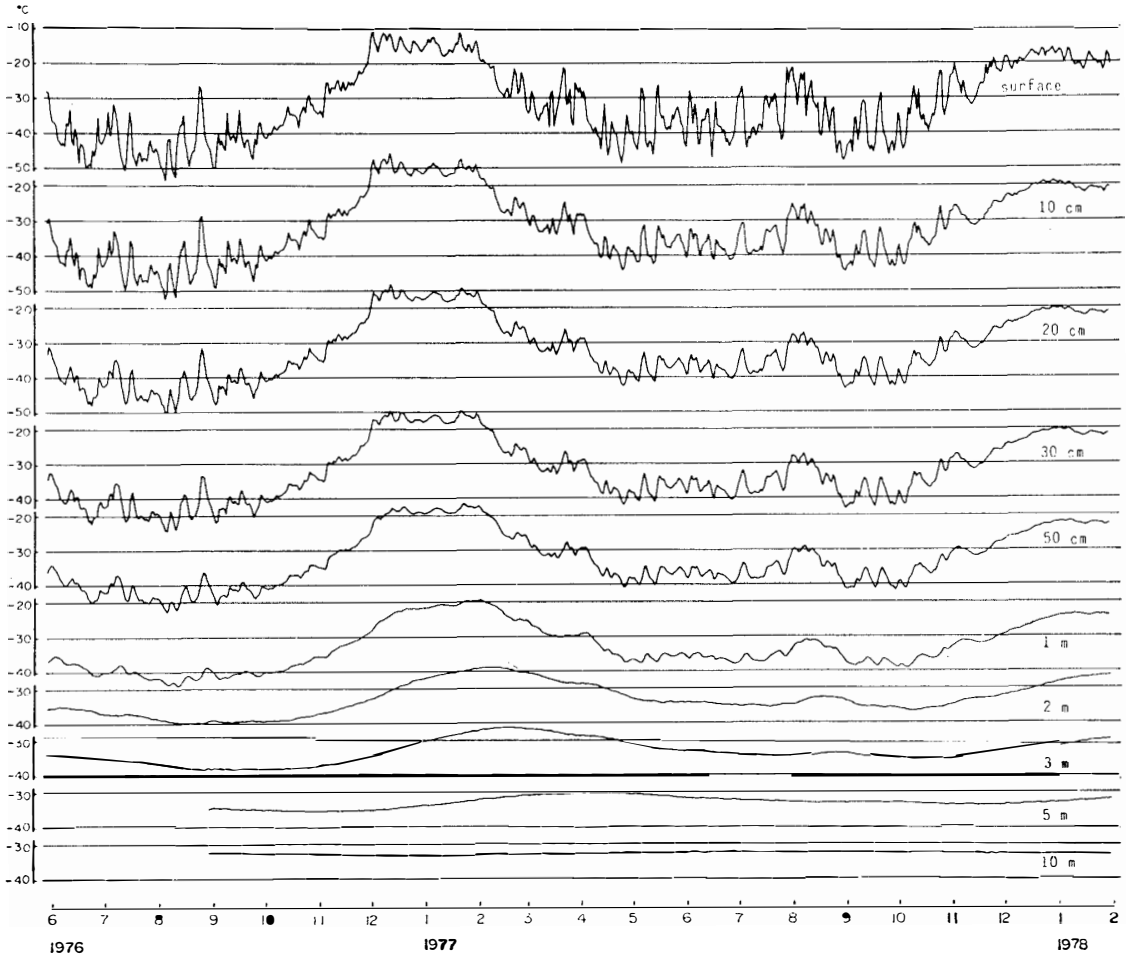

Fig. 9. Mean daily snow temperature at the surface, 0.1, 0.2, 0.3, 0.5, 1, 2, 3, 5 and 10 m.

At the snow surface the annual temperature variation has the amplitude of about 40 degrees. During winter there are temperature fluctuations of several days with the amplitude of about 20 degrees, which was due to the influence of climatic disturbances such as cyclones penetrating into the inland. As illustrated in Fig. 9 the mean daily surface temperature indicates gradual warming at the end of winter around October and fluctuations become small during summer. To find the periodicity of the snow surface temperature fluctuations, a spectral analysis technique (IWABUCHI *et al.*, 1978) based on the maximum entropy theory was applied to the hourly readings of surface snow temperatures. The power spectrum shown in Fig. 10 indicates significant peaks at periods of 7.3, 3.0, 1.0 and 0.5 days. In this analysis, the annual cycle was not resolved from a single year's data, but the presence of annual cycle is recognizable from Fig. 9.

To examine the propagation of temperature waves into the snow from the surface, a heat conduction equation will be solved under a simple sinusoidal variation of surface temperature as a boundary condition (CARSLAW and JAEGER, 1959; PATERSON, 1969). The surface temperature is given by,

$$T(0, t)=T_0+T_s \cos \omega t\,, \qquad (1)$$

where T is temperature, t the time, T_0 the mean annual temperature, T_s the amplitude and $\omega/2\pi$ the frequency of the surface temperature change as already shown at periods of 0.5, 1.0, 3.0, 7.3 days and 1 year in Fig. 10.

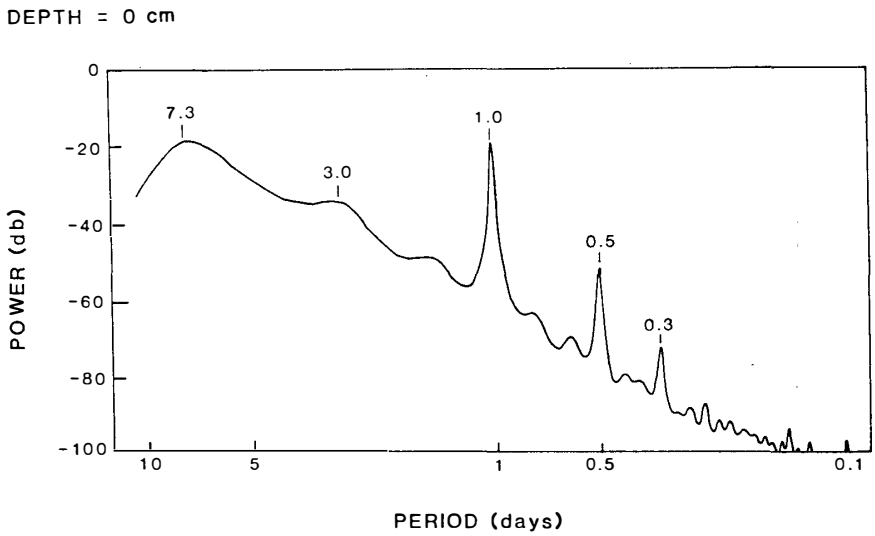

Fig. 10. Power spectrum of hourly snow surface temperature at Mizuho Station.

The temperature regime within a semi-infinite snow cover can be obtained by solving the following heat conduction equation:

$$k\frac{\partial T^2}{\partial z^2}=\frac{\partial T}{\partial t}\,, \qquad (2)$$

where k is the thermal diffusivity of snow and z the depth.

The solution of eq. (2) for the boundary condition given by eq. (1) is:

$$T(z, t)=T_0+T_s \exp\left[-z\left(\frac{\omega}{2k}\right)^{1/2}\right]\cos\left[\omega t-z\left(\frac{\omega}{2k}\right)^{1/2}\right]. \quad (3)$$

This solution shows, at first, that any variations of surface temperature attenuate with depth according to the factor of

$$\exp\left[-z\left(\frac{\omega}{2k}\right)^{1/2}\right].$$

Thus, the presence of the term $-(\omega)^{1/2}$ in the exponent means that rapid temperature fluctuations at the surface are more quickly attenuated than slower ones. In reality we find that diurnal temperature variations are attenuated to about 5% of their surface temperature at the depth of 50 cm, while the annual cycle is attenuated to about 2.5% of its surface amplitude, the annual temperature wave with the amplitude of 0.9°C, when it reaches 10 m depth. Therefore, it is seen that at most depths the annual temperature wave dominates over other shorter period variations.

Secondly, the speed of propagation of the temperature minimum or maximum is expressed as the phase term $z(\omega/2k)^{1/2}$, which has the effect that more rapid fluctuations are more rapidly transmitted. Thus, we find that, for example, at a depth of 1 m, the minimum of diurnal temperature variations occurs about one day after the minimum at the snow surface, while the minimum of the annual cycle propagates to 1 m depth in a time of about 18 days. These effects of selective attenuation and phase delay can be seen clearly from Fig. 9.

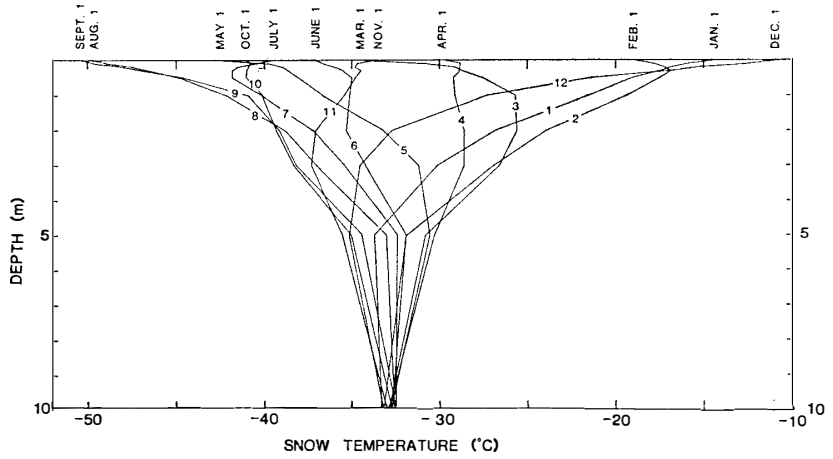

Fig. 11. Monthly snow temperature profiles at Mizuho Station in 1976–77.

Snow temperature profiles as a function of depth at the beginning of each month throughout the whole year are plotted in Fig. 11. The tautochrone of snow temperature profiles indicates rapid warming at the beginning of summer and rapid cooling at the end of summer; this situation is also to be seen in Fig. 9. This is typical 'coreless winter' temperature pattern, which is a characteristic feature in weather patterns in the interior of the Antarctic (LOEWE, 1969).

4. Characteristics of Thermal Cracks

Most of the thermal cracks observed on the snow surface are located on the glazed surface which is classified as the long-term hiatus form in surface features and is related closely to the absence of annual layers (WATANABE, 1978). The glazed surface with multi-yeared ice crust is distributed widely around Mizuho Station and developed on the upper part of snow mounds on the ice sheet surface where accumulated snow is scarcely found. Thermal cracks are usually visible on the glazed surface and exhibit polygonal patterns as shown in Fig. 12 and the cracks often exhibit parallel strips. Thermal cracks are also observed on the smooth surface without sastrugi; in this case, thermal cracks are almost in the pattern of parallel strips. Most of the thermal cracks are narrow in width, less than several centimeters, but thermal cracks wider than about 10 cm are frequently found. Figure 13 shows the vertical section of thermal crack in a trench wall at Mizuho Station; the maximum width of the thermal crack is about 10 cm and its depth below the surface is about 2.5 m. In general, most of thermal cracks observed are narrow, less than several centimeters in width, and are as shallow as 1 m in depth.

It is likely that occurrence of narrow thermal cracks in the surface snow layer

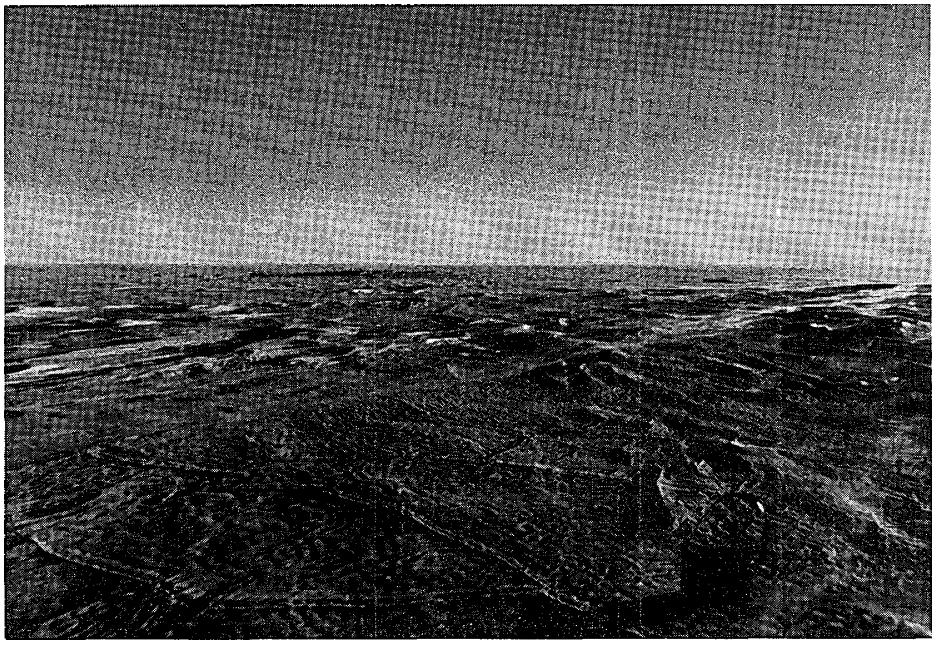

Fig. 12. Glazed surface and polygonal pattern of thermal cracks near Mizuho Station.

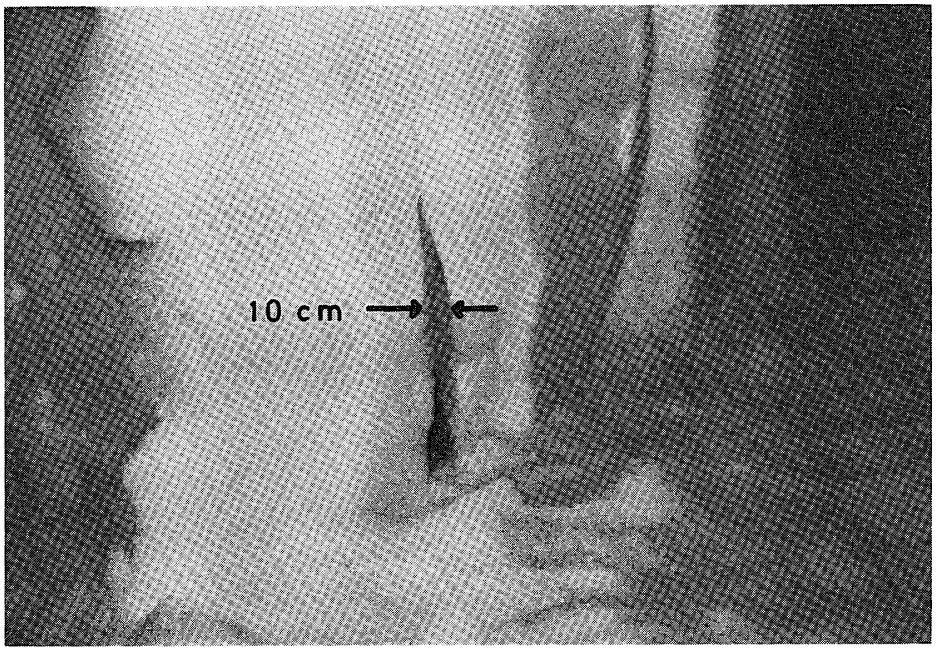

Fig. 13. Vertical section of thermal crack in a trench wall at Mizuho Station. The maximum width is about 10 cm and its depth is about 2.5 m below the surface.

was due to the result of thermal contraction when the surface temperature decreased and these narrow thermal cracks will open and close according to snow temperature fluctuations. We will describe in detail the characteristics of cracks of thermal origin in the following subsections.

4.1. Distribution of thermal cracks on the snow surface

It was mentioned that thermal cracks observed are located on the glazed surfaces. Then, the areal distribution of glazed surfaces should be shown in order to know the distribution of thermal cracks on snow surface. FUJIWARA and ENDO (1971) reported that along the traverse route of about 43°E between Syowa Station and the South Pole in 1968–69 the glazed surfaces were remarkably developed on the upper part of the mound formed on the katabatic slope between 70 and 72.5°S, whereas on the interior slope between 82 and 89°S the glazed surfaces were also found on the top of undulations. On the other hand, WATANABE (1978) pointed out that the glazed surface was developed in a region where the surface elevation was between 1800 and 3200 m. It can be considered that the glazed surface is formed in a belt-shaped zone with an interval of 10–20 km along the direction of prevailing wind. The average width of glazed surface in the direction normal to the prevailing wind seems to be a few km, while some of the most developed belts of glazed surface are a few 10's km in width. The occurrence of glazed surface becomes more often in the range of elevation from 2500 to 3100 m, and in the vicinity of the glazed surface in this area the surface is smooth and the patch-like glazed surfaces are seen.

The glazed surface is defined as the surface feature in long-term hiatus form which is related closely to the absence of snow accumulation in annual layers. Therefore, it should be expected that the glazed surface with thermal cracks as shown in Fig. 12 will be observed on the surface condition which shows no snow accumulation. Figure

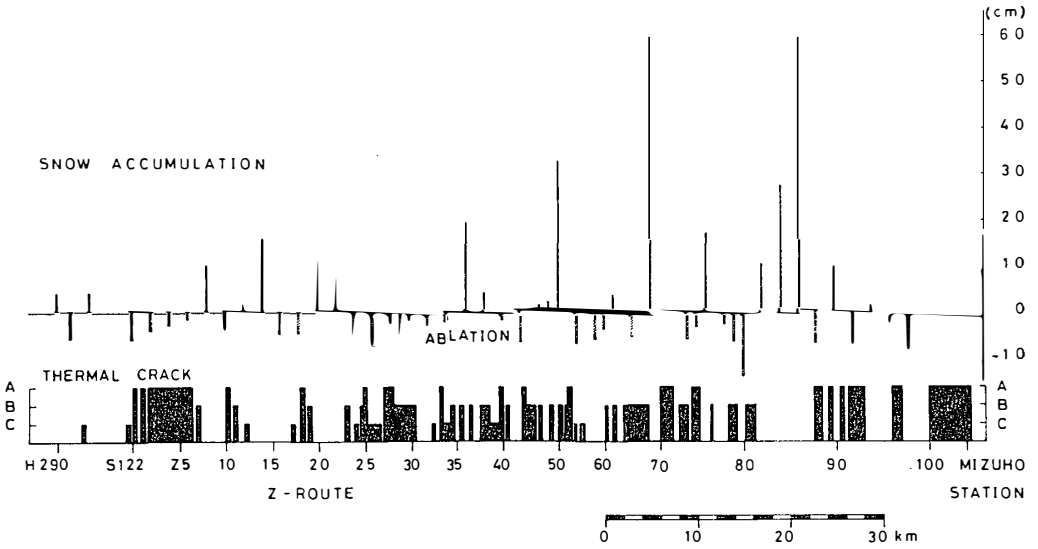

Fig. 14. Relation between snow accumulation and frequency of occurrence of thermal cracks observed along the Z-route between Mizuho Station and Station H290 midway between Syowa and Mizuho. Snow accumulation at every 2 km was measured from January 1976 to January 1977.

14 shows the relation between the snow accumulation measured by snow stakes at every 2 km and the frequency of occurrence of thermal cracks observed on the glazed surfaces along the route from Mizuho Station to Station H290 situated midway between Syowa and Mizuho. The frequency of occurrence of thermal cracks is defined by number density of crossed thermal cracks within 1 km long survey line, and classified into three cases; the number density is more than 50 (A), 10 to 50 (B) and less than 10 (C). It is clear from Fig. 14 that the thermal cracks could be observed on the glazed surfaces where there is no snow accumulation or ablation at the surface, and that the higher number density of thermal cracks is remarkably observed in high snow ablation area, while no thermal crack was observed where there is much snow accumulation, namely depositional form in surface features.

Around Mizuho Station a large area of glazed surface with thermal cracks occupies the surface snow cover and the thermal cracks indicate a particular pattern in the form of polygons or parallel strips as illustrated in Fig. 15. The observation of the pattern of thermal cracks on the surface snow cover within the seismograph array was carried out in November 1976 when snowquakes were highly active due to fracturing of the surface snow cover. As seen in Fig. 15 the spacing of individual crack shows various length. In the form of parallel strips, most of crack spacing was about 5 to 20 m, while the crack spacing in the pattern of polygons was mostly a few meters. Since July 1970 the observation of pattern of thermal cracks has been carried out in the same area of glazed surface which was kept intact near seismograph No. 2 as shown by a square area in Fig. 15. Figure 16 shows the patterns of thermal cracks which were observed on four occasions, July 1970, January 1971 (WATANABE and YOSHIMURA, 1972), December 1971 (YAMADA, 1975) and January 1977 (NISHIO, 1978). It can be seen that between July 1970 and December 1971 nearly the same polygonal thermal cracks appeared and in places several cracks grew and crossed other cracks, and during

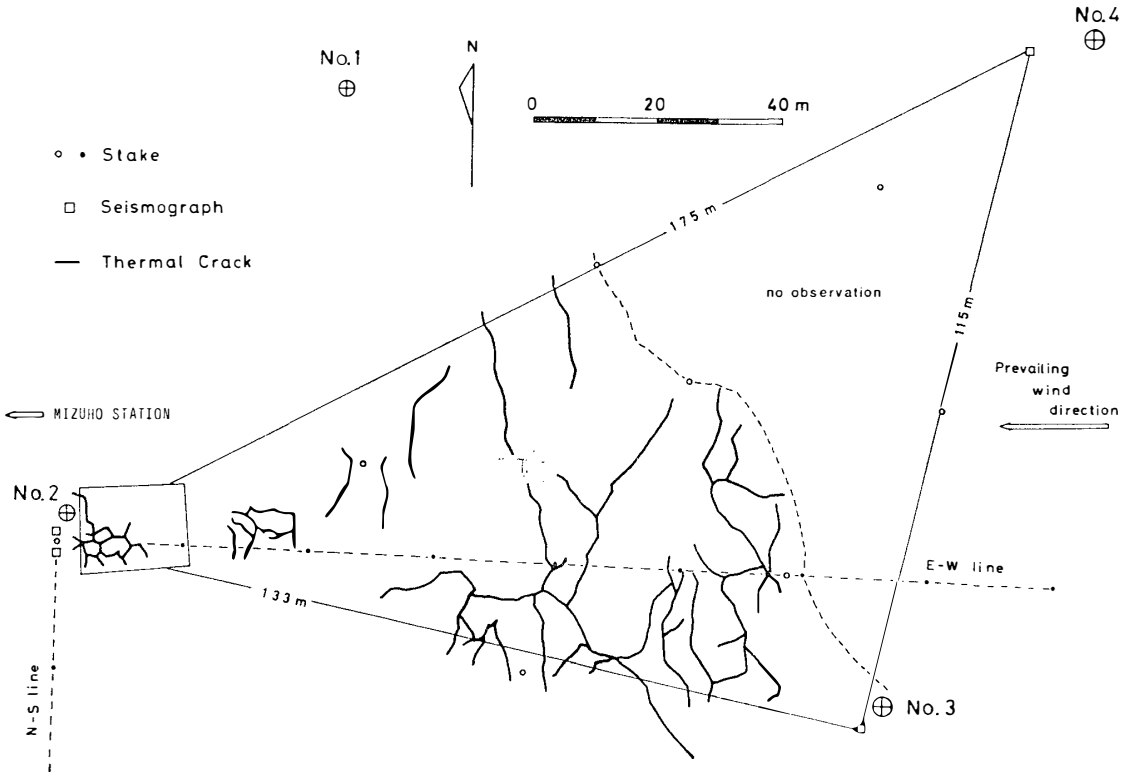

Fig. 15. Pattern of thermal cracks on the glazed surface within the array of seismograph. Details of thermal crack in the square near seismograph No. 2 have been observed since July 1970.

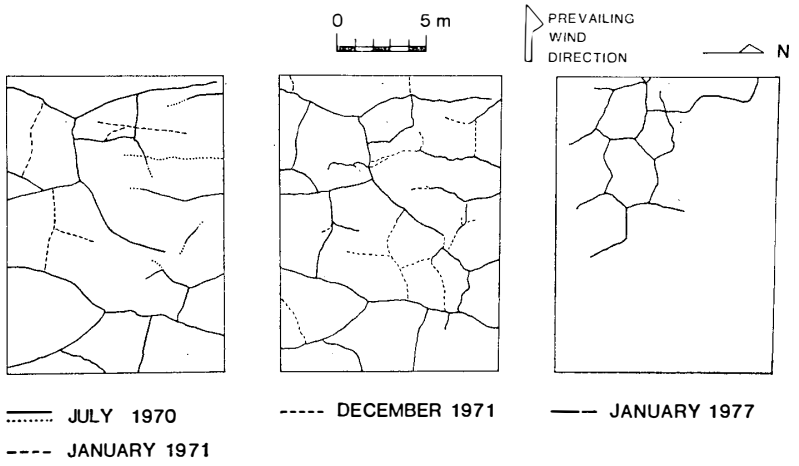

Fig. 16. Pattern of thermal cracks in the square observation area (Fig. 15). No snow was deposited between July 1970 and December 1971, but about 50 cm of snow was deposited from December 1971 to January 1977.

that period no accumulation of snow was observed by stakes installed at four corners of the square observation area. However, the pattern of thermal cracks changed between December 1971 and January 1977 and about 50 cm of snow accumulated during this period; the change in the pattern of thermal cracks within about 5 years may have resulted from the snow accumulation on the glazed surface.

Figure 17 shows the vertical section of the uppermost 1.5 m of the snow cover at a distance of about 20 m in the lee-wind side of the thermal cracks observation area in Fig. 16. Although no thermal crack was found on the snow surface, there existed many thermal cracks at a depth of about 50 to 60 cm. The fine-grained surface snow layer of 50 to 60 cm in thickness with a density of 0.4 g/cm^3 is equivalent to the amount of snow accumulated on the glazed surface in the square observation area of pattern of thermal cracks. Thus, it is found that the pattern of thermal cracks

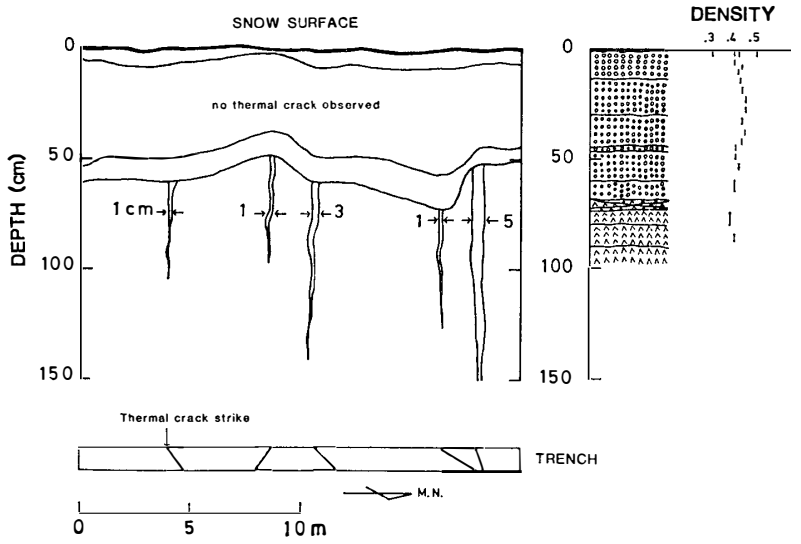

Fig. 17. Vertical section of thermal cracks in the trench wall which is located about 20 m in the leeward of the thermal crack observation square in Fig. 15.

on glazed surfaces is maintained and cracking is well propagating in response to thermal strain due to snow temperature fluctuations. Once thermal cracks on glazed surface are covered with a thick snow layer such as barchan or dune, the formation of thermal cracks within the snow cover is unlikely unless the thermal stresses attain large enough to initiate cracks (see Fig. 17). Once a thermal crack is initiated in the snow cover, we would expect stress concentration at the tip of the crack and cracking will well propagate even under lower thermal stresses. There was a surface snow cover of about 50 cm thick in January 1977 as shown in Fig. 16, and the formation of thermal cracks in this snow cover will take place when the thermal stress is considerably large.

4.2. Variation of width of thermal cracks

Temperature waves with various amplitudes and periods propagate into the snow cover. This will cause the expansion and contraction of the surface snow cover. In considering the fracture of snow cover without cracks, we shall be concerned not only with the average thermal stresses in the snow cover, but with the maximum thermal stresses for the initiation of fracture. Cracking will occur when the maximum thermal stress exceeds the fracture strength of the snow cover. Once cracking is initiated in the snow cover, we should expect the progress of stress concentration at the tip of crack to allow it to propagate well beyond the region in which the thermal stress attains less than the maximum thermal stress to initiate crack. Thus, in the snow cover with many thermal cracks, fracture will occur not only in excess of the maximum thermal

stress, namely the tensile strength of snow, but also in the minimum stress required to propagate a crack.

On the other hand, once thermal cracks in the snow cover were formed, it may be possible that thermal cracks close when the temperature increases during the summer, and again thermal crack is formed when the temperature decreases and the stress again exceeds the fracture strength of snow.

As was mentioned earlier, the length of two reference points across thermal crack was measured by using a vernier calliper. Here we treat the variation of the length as the variation of width of thermal crack. As shown in Figs. 18a and 18b, the length of sides of $\overline{AB}$, $\overline{CD}$, $\overline{BC}$ and $\overline{AD}$, and of diagonals of $\overline{AC}$ and $\overline{BD}$ in the square illustrated in the Fig. 3b were measured once a day. The variation of length of side across thermal crack such as $\overline{AB}$, $\overline{CD}$, $\overline{AC}$ and $\overline{BD}$ is remarkably depending on the variation of the surface snow temperature. During the winter from June to September the length across thermal crack became longer with decreasing temperature and the fluctuations of distances within several days were a few mm. From the beginning of October the length across thermal crack quickly decreased and shortened by 5–8 mm with the temperature increasing during the summer. On the contrary, the length of $\overline{BC}$ and $\overline{AD}$ on both sides of the thermal crack did not follow the variation of the snow surface temperature. Thus, it is considered that the variations of length across thermal crack indicate the variation of width of thermal crack due to temperature variations.

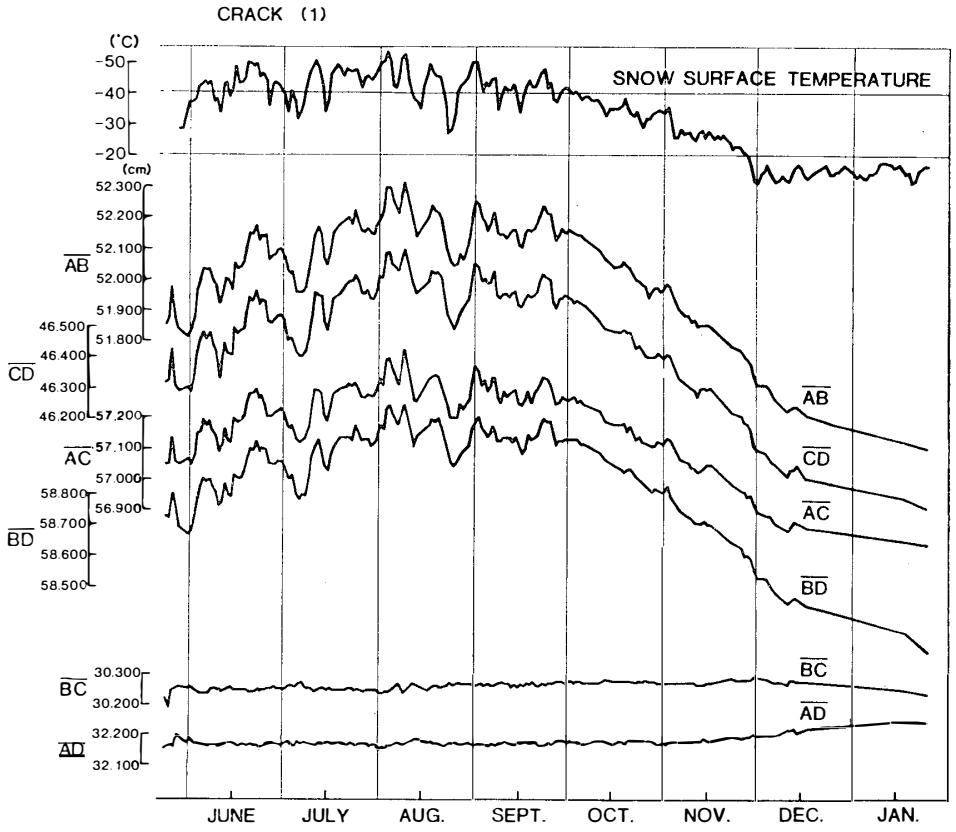

Fig. 18a. Variations of length of sides and diagonals of the square across the thermal crack No. 1 in Fig. 3b.

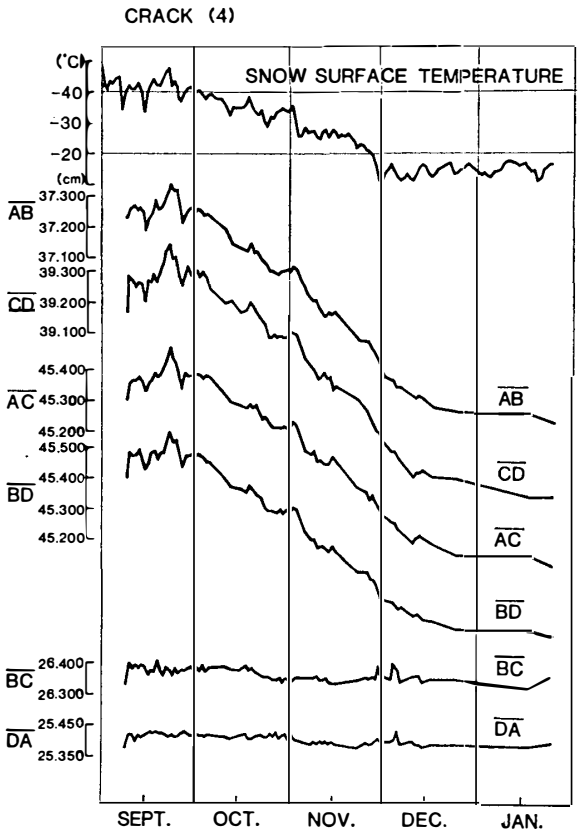

Fig. 18b. Variation of length of sides and diagonals of the square across the thermal crack No. 4 in Fig. 3b.

We shall discuss the variations of width of thermal crack and the character of the strain rate field surrounding the crack. Figure 19 shows a field of thermal cracks at spacing of l. Thermal cracks will open and close according to snow temperature fluctuations, but the width of opening depends on the degree of expansion and contraction of snow between thermal cracks. Near the surface, immediately on the boundary of a thermal crack, the snow is free to expand and contract in response to fluctuations of snow temperature, but any thermal straining of expansion and contraction is attenuated with depth with regard to the heat conduction properties already mentioned and is also attenuated with distance inwards from a thermal crack according to the Saint Venant's principle concerning edge effects. Attenuation of temperature wave with depth depends on frequency and occurs according to $\exp[-z(\omega/2k)]^{1/2}$. Here, skin depth of z_0 is defined as $z_0=(2k/\omega)^{1/2}$ representing the depth at which temperature effects are attenuated by a factor of $1/e$. We shall use this skin depth as a characteristic distance for the attenuation of thermal effects in the z direction, and shall make the further assumption that it also characterizes the attenuation with distance inwards from a thermal crack in the x direction as suggested by SANDERSON (1978). This is a way of expressing the principle that edge effects generally die away from a free boundary. This means that we can approximately express the strain rate field as a function of x and z:

$$\dot{\varepsilon}_{xx}(x, y)=(\dot{\varepsilon}_{xx})_0 \exp(-z/z_0) \exp(-r/z_0) . \qquad (4)$$

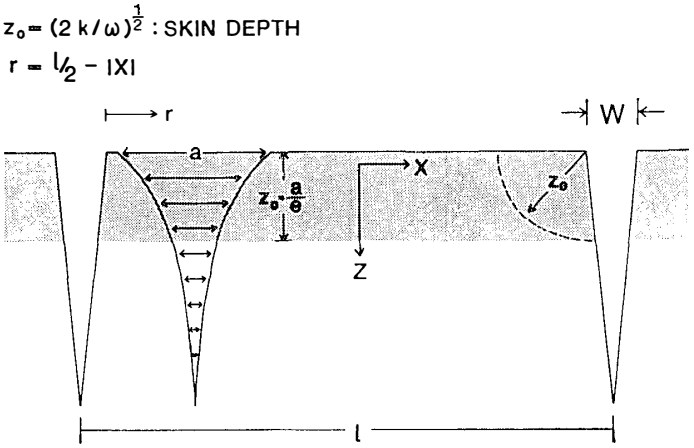

Fig. 19. A schema illustrating strain rate field surrounding thermal cracks undergoing thermal strain in the snow cover near the surface. Appreciable strain occurs within a region of order z_0 surrounding a thermal crack.

And

$$r=l/2-x\,,$$

is the distance away from a crack. $(\dot{\varepsilon}_{xx})_0$ is the strain rate which a free snow mass would undergo if subjected throughout to the snow surface temperature fluctuation, that is, $(\dot{\varepsilon}_{xx})=\alpha\partial T/\partial t$, where α is the linear expansion coefficient of snow given by YAMAJI (1957),

$$\alpha=5.4\times10^{-5}+1.8\times10^{-7}T\,, \tag{5}$$

where T is the snow surface temperature.

We can now calculate the rates of opening of thermal cracks. Taking the origin of coordinates in the middle of spacing l as a stationary point, and then integrate the strain rate with respect to x to find the rate of movement V_e of width of thermal crack. This gives, for the snow surface, $z=0$,

$$\begin{aligned} V_e&=2\int_0^{1/2}\dot{\varepsilon}_{xx}\,(x,0)\mathrm{d}x \\ &=2(\dot{\varepsilon}_{xx})_0 z_0[1-\exp(-1/2z_0)]\,, \end{aligned} \tag{6}$$

and provided that $l\gg z_0$, that is, the thermal crack spacing is by far greater than the skin depth because most of thermal crack have the spacing of more than several meters as mentioned in the previous subsection, then we can write the velocity of opening and closure of thermal crack, as

$$V_e=2(\dot{\varepsilon}_{xx})_0 z_0\,. \tag{7}$$

For the maximum width W of thermal crack we can write the following equation in the same way,

$$W=2(\varepsilon_{xx})_{max}\,z_0\,, \tag{8}$$

where $(\varepsilon_{xx})_{max}$ is the maximum strain which a free snow mass should undergo if subjected throughout to the snow surface temperature change, that is $(\varepsilon_{xx})_{max}=\alpha\cdot\Delta T$, where ΔT is the snow surface temperature change.

As derived from eqs. (7) and (8), the rate of movement of width of thermal crack V_e and the maximum width of thermal crack W have a function of only skin depth z_0. Table 1 shows a comparison of calculated and measured values of skin depth, rate of movement of crack edge and the maximum width of two thermal cracks, crack (1) and crack (4). There are many cases in thermal fluctuation with different skin depths, but for the purpose of accounting for the variation of width of thermal crack we dealt with two cases of snow surface temperature, daily oscillation with an amplitude of 13.5°C, and annual oscillation with an amplitude of 40°C, for which the associated skin depth is about 20 and 300 cm respectively. Table 1 clearly indicates that the variation of width of thermal crack is strongly depending on the air temperature waves, and shorter-period wave gives the more rapid but smaller opening and closing, and longer period wave gives the slower but larger opening and closing.

Table 1. Skin depth, rate of movement of thermal crack edge and the maximum width of thermal crack.

	Diurnal cycle			Annual cycle		
	November 29–30, 1976 (1 day)			August 1976–January 1977 (180 days)		
		Crack No. 1	Crack No. 4		Crack No. 1	Crack No. 4
	Calculated	Measured		Calculated	Measured	
Skin depth z_0 (cm)	17	20		317	300	
Rate of movement of thermal crack edge V_e ($\times 10^{-8}$ cm·hour^{-1})	2.48	4.86	7.70	1.56	1.97	1.80
Maximum width of thermal crack W (cm)	0.047	0.048	0.086	0.96	0.84	0.76
Amplitude of snow surface temperature ΔT (°C)	13.5			40.0		

During repetition of opening and closing of thermal cracks, narrow cracks may grow wider owing to the progress of snow metamorphism of the wall of thermal crack in the vertical direction because hoarfrost formed by sublimation was observed on the wall.

4.3. Thermal cracks and snowquake activities

The variation of width of thermal cracks is dependent on the thermal expansion and contraction induced by temperature change, also the formation and growth of thermal cracks are strongly associated with snowquake activity. Thermal cracks already existed are found to be remarkably influenced by the temperature waves, that is, the opening and closing of thermal crack, and the formation of thermal crack and the propagation of a tip of thermal crack may cause snowquakes when the thermal stress induced by snow temperature variations exceeds the fracture strength of the snow cover.

Figures 20a and 20b show the daily variations of length of sides and diagonals of the square across the thermal cracks (1) and (4) respectively. These variations are considered to correspond to the variation of width of thermal crack. Snow surface temperature and number of snowquakes are also shown in the figures. Figures 20a and 20b show considerable daily variations of the snow surface temperature during the summer. When the temperature is decreasing after the maximum in the early afternoon, the thermal crack begins to open and becomes about 0.5–0.8 mm wide till the temperature reaches the minimum. The snowquake begins in accompany with the rapid temperature decrease a few hours later after the maximum snow surface temperature and during the temperature decrease the swarm-like snowquakes occur till the temperature reaches the minimum. When the snow surface temperature was increasing, snowquakes did not occur. Thus, it is evident that the opening of thermal crack and the initiation of snowquakes are closely related to the thermal contraction of the snow cover as the result of decrease of the snow surface temperature. However, the initiation of snowquakes should be caused by the new formation of thermal crack in the snow cover or the propagation of a tip of existing thermal crack. Figure 21 shows a new thermal crack just after the occurrence of snowquakes when the snow surface temperature was about −50°C. The new thermal crack, about 0.5 mm wide,

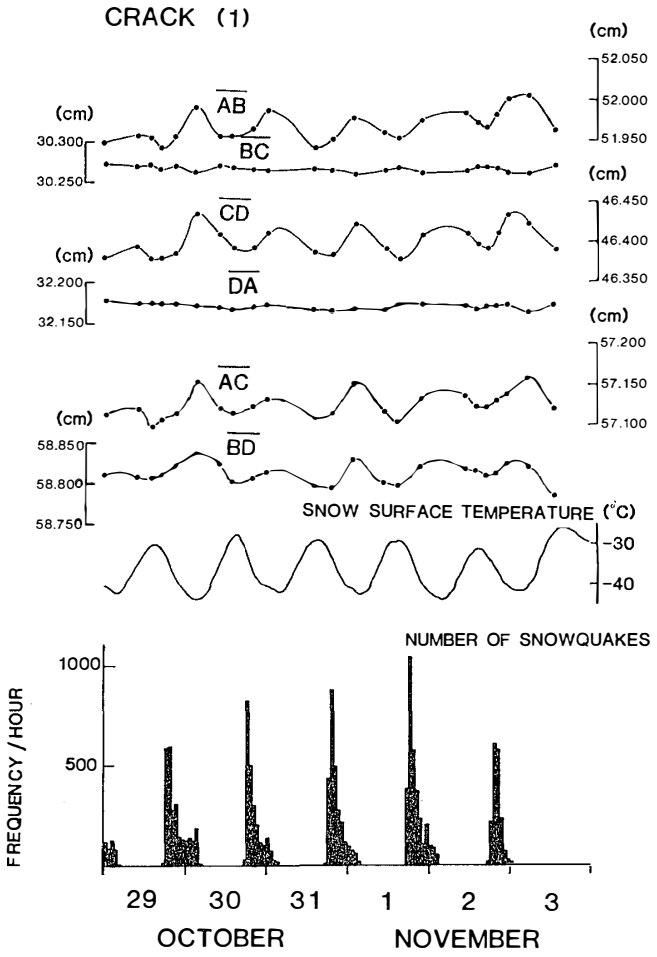

Fig. 20a. Daily variations of length of sides and diagonals of the square across the thermal crack No. 1 in Fig. 3b, snow surface temperature and number of snowquakes.

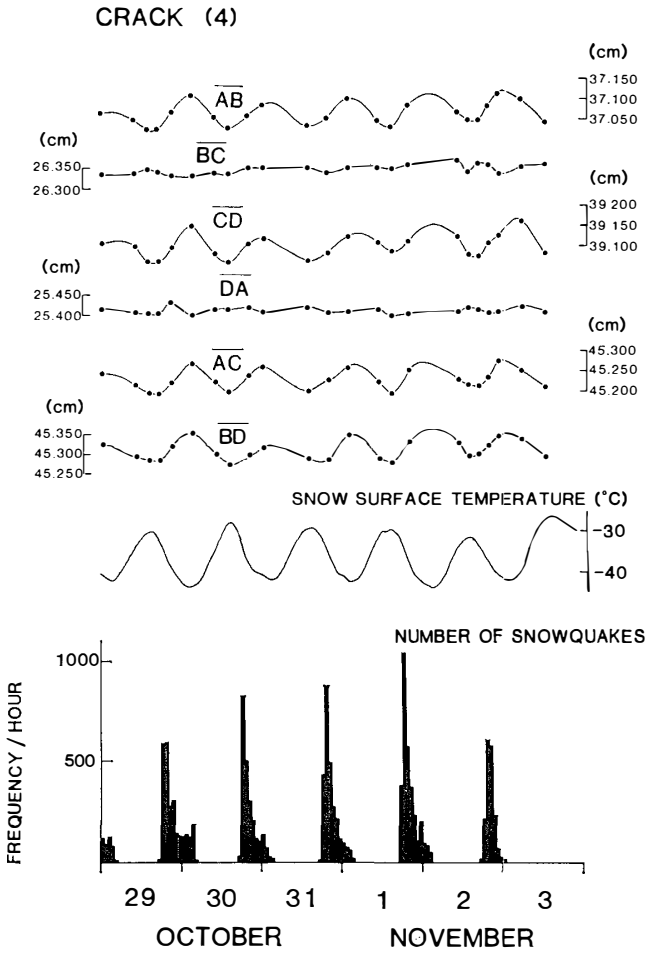

Fig. 20b. Daily variations of length of sides and diagonals of the square across the thermal crack No. 4 in Fig. 3b, snow surface temperature and number of snowquakes.

about 20 cm deep and about 3 m long, was formed on the glazed surface on August 30, 1976. This observation leads to a possible explanation of the initial stage of formation of thermal crack and of the occurrence of snowquakes observed as the result of detecting elastic waves radiated by the fracture of the snow cover due to thermal contraction. Another cause of occurrence of snowquake is explained by the fracture which was due to the process of stress concentration at a tip of already existent thermal crack.

In order to know whether the opening and closing of thermal crack are associated with extensional faulting (tensile cracking) or with slip faulting, calculations were made on the deformation of triangle across a thermal crack, such as crack (1) shown in Fig. 3b. It was assumed that the strain parameters of the triangle indicate those of the thermal crack. To calculate the strain parameters in each triangle, the JAEGER's method (1969) is used as the rate of deformation of a circumscribed circle of an unstrained triangle into a strain ellipse caused by a homogeneous strain. Coordinates of each vertex of triangles in the square across thermal crack are determined with reference to appropriate vertex of triangle in the case of each measurement of sides of the square as shown in Fig. 3b. Hence, the shape of the strain ellipse and the rotation

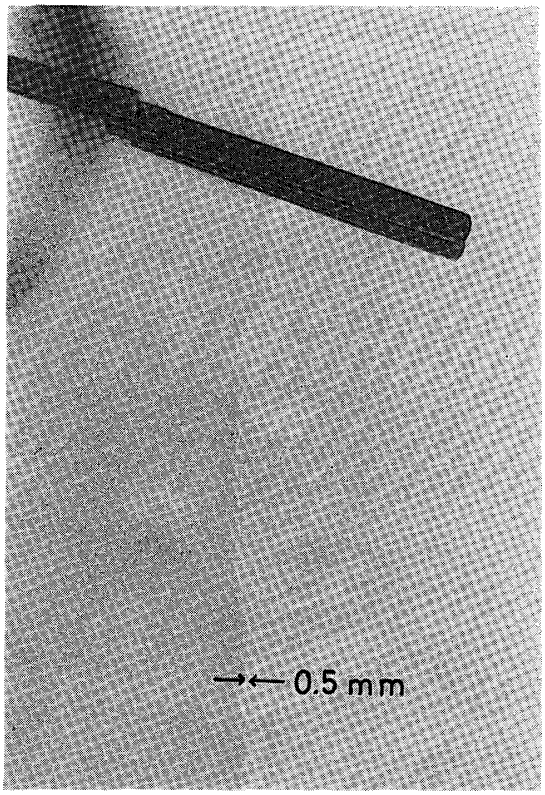

Fig. 21. A new thermal crack about 0.5 mm wide, ca. 20 cm deep and ca. 3 m long, which was formed on the glazed surface on August 30, 1976 just after the occurrence of snowquakes at the snow surface temperature of −50°C.

of the principal axis of the strain can be calculated. Taking the radius of the circumscribed circle of an initial triangle as the unity, and the length of major and minor axis of the strain ellipse being A and B respectively, the parameters of deformation of triangle such as principal strain rate, dilatation, maximum shear strain rate and rotation of principal axis of the strain, were computed as a function of A and B. As the result of calculation of the values of A and B of each triangle, the following strain parameters were obtained:

$\dot{\Delta}$: Rate of dilatation in the area of a triangle per hour, calculated from $\dot{\Delta}=AB-1$.

$\dot{\varepsilon}_1$, $\dot{\varepsilon}_2$: Principal strain per hour, calculated from $\dot{\varepsilon}_1=A-1$ and $\dot{\varepsilon}_2=B-1$. The positive sign indicates the tensile strain rate and the negative for compressive. The principal strain rate of $\dot{\varepsilon}_1$ and $\dot{\varepsilon}_2$ respectively the algebraically maximum and minimum values among the strains in the whole directions.

α: Azimuth clockwise from north of the principal axis of the strain $\dot{\varepsilon}_1$.

$\dot{\omega}$: Rate of counterclockwise rotation of the principal axis of the strain per hour.

$\dot{\gamma}_{max}$: Maximum shear strain rate per hour, calculated from $\dot{\gamma}_{max}=(A^2-B^2)/2AB$. Its direction is $\pm 45°$.

Figure 22 shows the calculated strain parameters of the triangles in the square across the thermal crack (1) from October 29 to November 3. In Fig. 22, the daily variations of the dilatation $\dot{\Delta}$, the maximum principal strain rate $\dot{\varepsilon}_1$, the minimum principal strain rate $\dot{\varepsilon}_2$, the direction of principal axis of the strain α, the rotation of

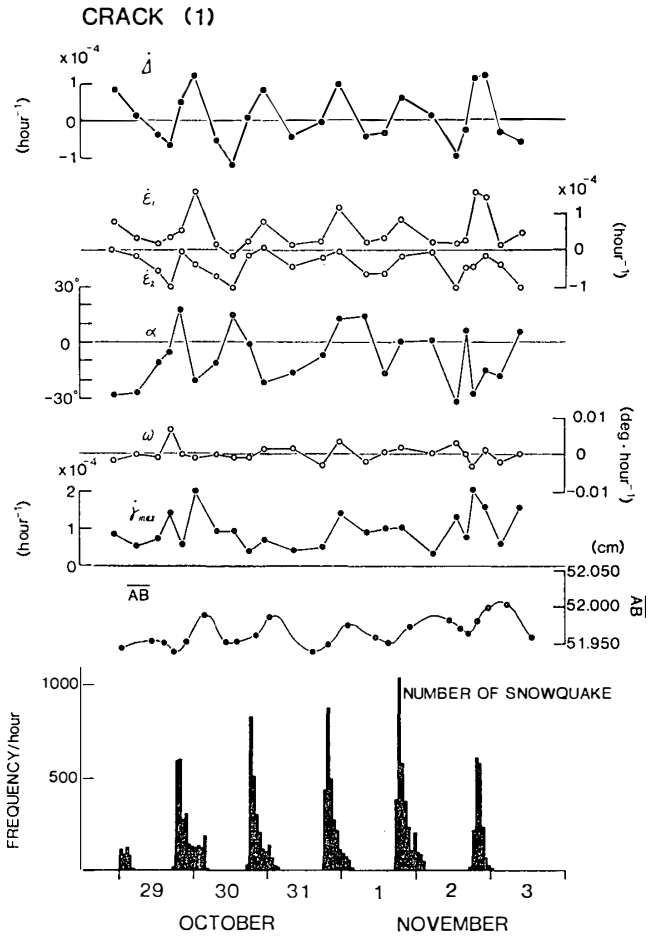

Fig. 22. Daily variations of the dilatation $\dot{\Delta}$, the maximum principal strain rate $\dot{\varepsilon}_1$, the minimum principal strain rate $\dot{\varepsilon}_2$, the direction of principal axis of the strain α, the rotation of the principal axis $\dot{\omega}$ and the maximum shear strain rate $\dot{\gamma}_{max}$ of triangles in the square across the thermal crack No. 1. The side $\overline{AB}$ of the square and the number of snowquakes are also shown.

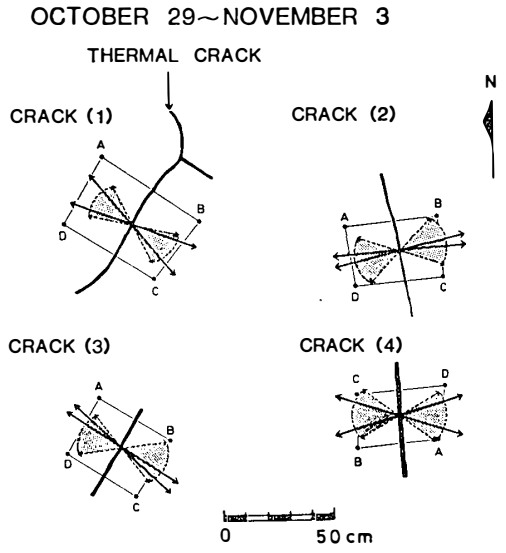

Fig. 23. Direction of principal axis of the strain (tensile strain) during the occurrence of snowquakes. The direction between two solid-line arrows indicate the tensile strain during the snowquake swarm and the daily variations of principal axis are also shown in the hatched area.

the principal axis $\dot{\omega}$ and the maximum shear strain rate $\dot{\gamma}_{max}$ are shown together with the length $\overline{AB}$ and the number of snowquakes. The dilatation $\dot{\Delta}$ becomes larger and the maximum principal strain rate $\dot{\varepsilon}_1$ of the tensile strain rate is also increasing during the occurrence of snowquakes from the early evening to the early morning every day.

The direction of the principal axis of the strain α in the tensile strain during the occurrence of the snowquake swarm indicates the tendency of the direction perpendicular to the strike of thermal crack. As seen in Fig. 23, the direction of the principal axis of the strain is indicative of the tensile strain and perpendicular to the strike of the thermal crack for the cases of cracks (1), (2), (3) and (4). This is evident that during snowquake swarm the tensile stress due to thermal contraction may be applied to thermal crack perpendicular to the strike and the tensile cracking may take place at the tip of thermal crack.

5. Characteristics of Snowquake Activities

KAMINUMA and TAKAHASHI (1975) observed snowquakes with one vertical component seismograph at Mizuho Station on September 10–27, 1973. They reported that many snowquakes, mostly of swarm type, were recorded, and that these swarms occurred in the nighttime when the air temperature was below −35°C, and the falling rate of air temperature was −2.5°C/hour for a short period, or about −1°C/hour when the falling of air temperature continued for a few hours. When the largest swarm was recorded, sound generated by snowquakes was heard and many thermal cracks were recognized on the snow surface around the source area of the sound. Therefore, the depth of the snowquake swarm was estimated to be very shallow. Some snowquakes were interpreted to have been originated from the upper snow layers quite near the surface.

From their study of snowquakes at Mizuho Station, it was expected that the snowquake activity would be closely associated with the fracture of snow cover such as thermal cracks due to thermally induced stress near the snow surface. But the mechanism of generation of snowquakes was still unsolved and hence the detailed investigation of the snowquakes was designed to be carried out by using three vertical-component seismographs in the array of tripartite.

5.1. General feature of snowquake activities

From June 8, 1976 to January 11, 1977, three vertical component seismographs were in operation at Mizuho Station. The trace amplitude larger than 2.0 mm in the recording chart was adopted as the snowquake, because the ground noise originated from artificial sources such as the power supply generator was large. Solid horizontal lines in Fig. 24 indicate observation time during which period snowquakes are detected on seismographs. The daily observation covers the period from June 1976 to January 1977. The date in the column gives from noon to noon of two successive days; for example, on June 11–12 the observation duration of snowquakes was from about 1400 LT June 11, through the midnight, till about 1100 LT of June 12, but the solid line does not indicate the frequency of occurrence of snowquakes.

From Fig. 24 three characteristic features of snowquake occurrence are clearly distinguished: (1) during the midwinter from June to August, the occurrence of snowquakes is irregular, (2) from September to November, the snowquake activity indicates the daily occurrence between the early evening and the early morning through midnight, and (3) at the end of November, when the summer began, snowquakes ceased

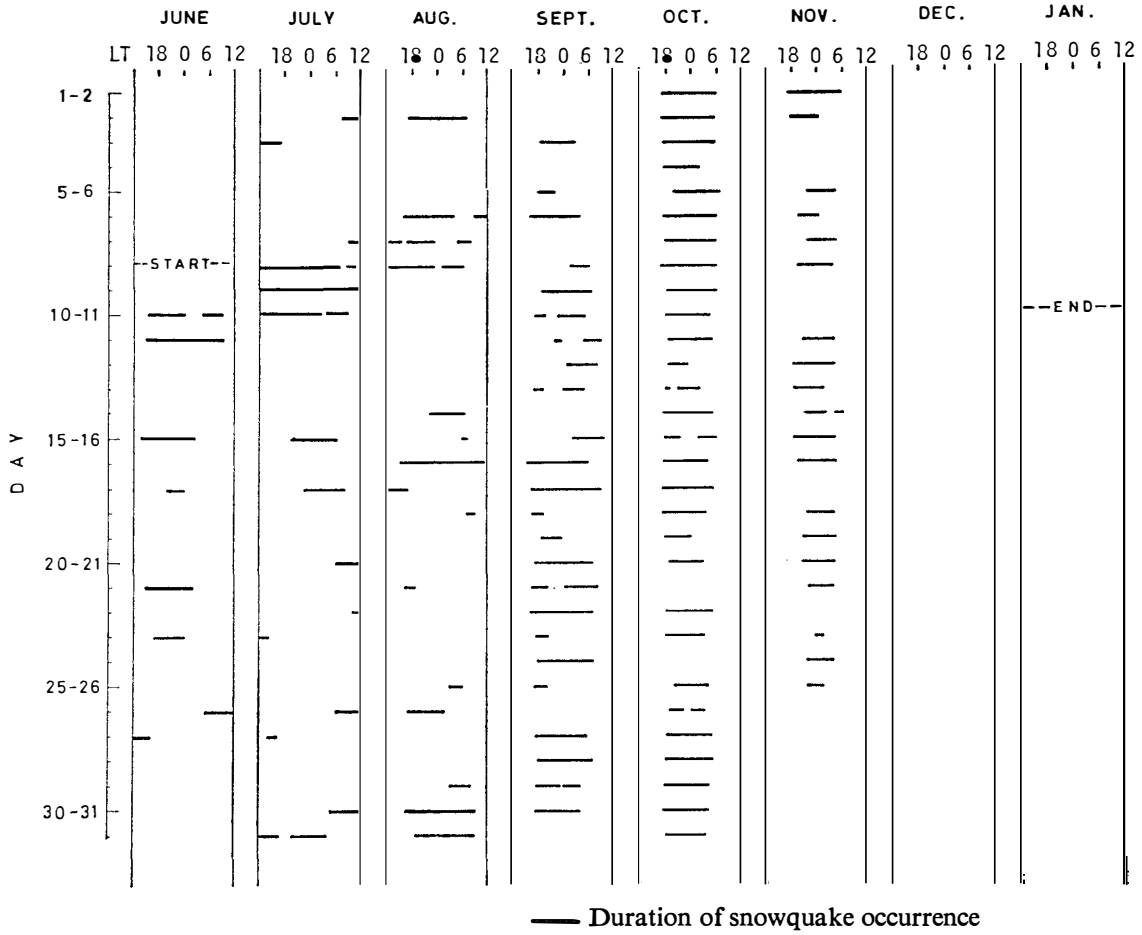

Fig. 24. Daily occurrence of snowquakes detected with seismographs.

and was not observed till the early January. This pronounced seasonal variation of snowquake occurrence must be related to the variation of snow temperature and the mechanical behavior of snow, for instance, such as the fracture strength having a temperature dependence.

During the midwinter when the snow temperature was mostly lower than −40°C as in the case of (1) in the previous paragraph, the snowquake started without exception immediately after the decrease in snow temperature. As was mentioned in Section 3, the surface temperature during winter fluctuated with the period of several days with an amplitude of about 20°C. This resulted from the warming and cooling which was due to climatic disturbances such as the penetration of low pressure into the inland around Mizuho Station. After the passing of low pressure, the snow surface temperature decreased under the influence of high pressure system and the snowquakes began to occur.

On the contrary, from the end of winter, in the case of (2), the diurnal surface temperature variations with an amplitude of 10–15°C became prominent because the snow surface was heated by the daily solar radiation change which depends on the sun's altitude. A few hours later after the maximum surface temperature around midday, the snowquake began to occur and during the decrease of snow surface temperature the snowquake swarm continued to occur till the temperature reaches the

minimum. From September to November snowquake swarm occur almost everyday, especially in October the snowquake swarm occurred everyday except two days.

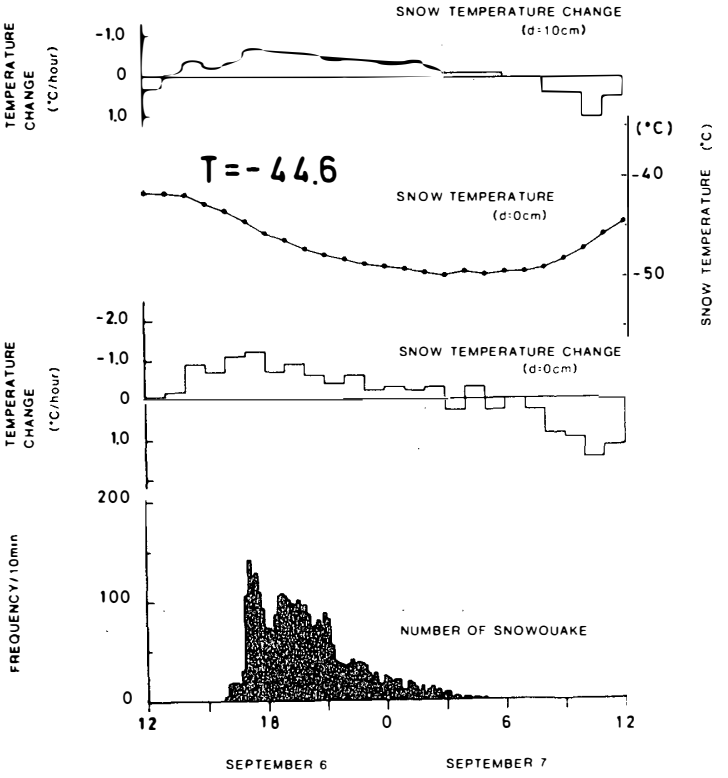

Fig. 25a

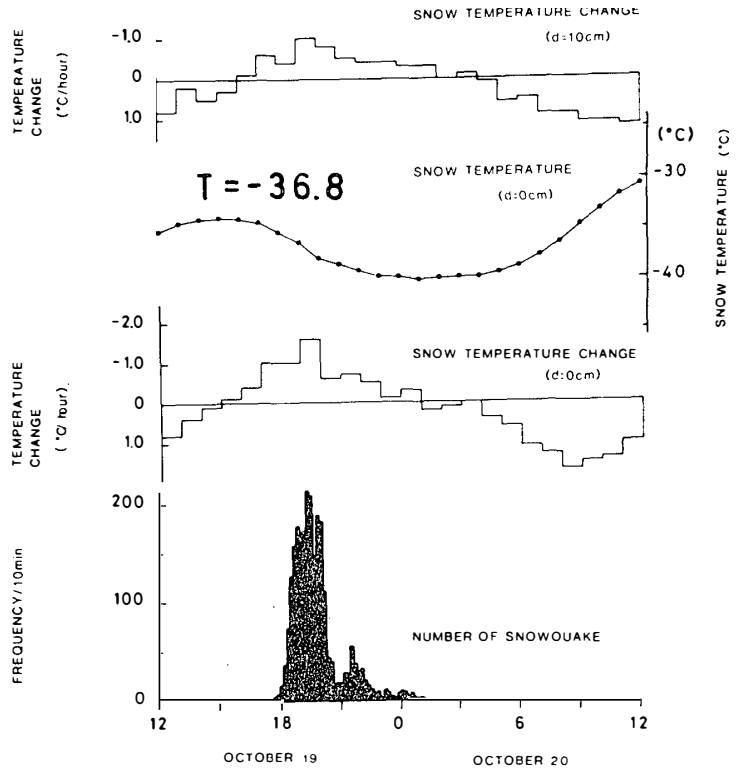

Fig. 25b

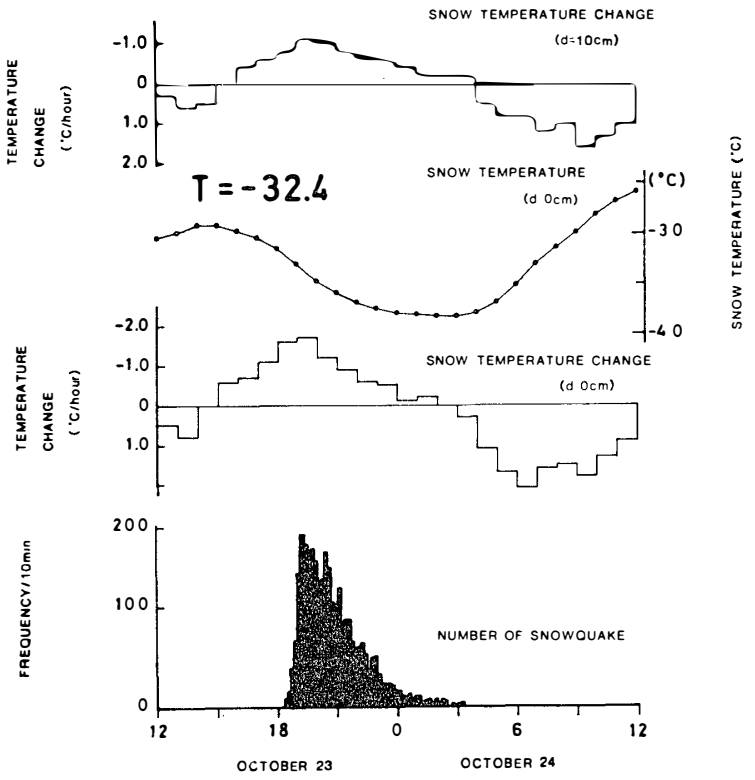

Fig. 25c

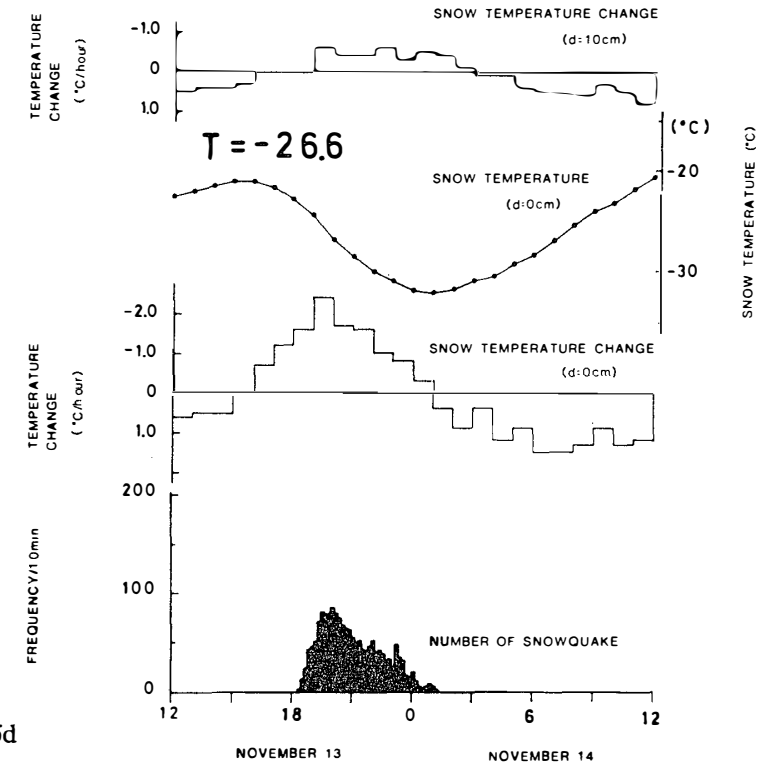

Fig. 25d

Fig. 25. Hourly range of snow temperature change at 10 cm, hourly snow surface temperature, hourly range of snow surface temperature change and the number of snowquakes per 10 min.

In the case of (3) at the end of November, although the diurnal variations of snow temperature were noticeable, the snowquake activity died suddenly. The mechanical behavior of snow such as the fracture strength depends greatly upon the temperature (BUTKOVICH, 1954). When the snow temperature is rising during the summer, the snow can undergo ductile deformation before the tensile stress due to thermal contraction exceeds the tensile strength of snow. Therefore, snowquake activity was finished in the summer.

Relation between the variation of snow temperature and the snowquake activity will be discussed in detail. Figures 25a–25d show 4 cases of relationship between the daily variation of snowquake activities and the snow temperature changes: during September 6–7 the daily mean snow surface temperature was −44.6°C, it was −36.8°C on October 19–20, −32.4°C on October 23–24 and −26.6°C on November 13–14. As a measure of snow temperature variation the hourly changing ranges of snow temperature at the surface and 10 cm depth are shown. As a measure of snowquake activity, recorded events with trace amplitude larger than 2.0 mm were counted within 10 min intervals. The total number of events thus counted was about 3340 on September 6–7, 2450 on October 19–20, 2790 on October 23–24 and 1630 on November 13–14. This will suggest that the total number of events depends on the daily mean snow temperature and is associated with the release of thermally induced strain energy. The release of strain energy will be discussed in detail in a later section.

Figures 25a–25d cleary show that the snowquake activity is strongly related to the snow temperature change at the surface rather than at 10 cm depth. A few hours after the maximum of the snow surface temperature, snowquake begins to occur and the activity rapidly reaches the maximum with around hundred events per 10 min. Active snowquakes are closely related with the lowering surface temperature which gives the high thermal stress to cause the fracture of surface snow cover. After the culmination of snowquake activity, it gradually became quiet around the minimum of the snow surface

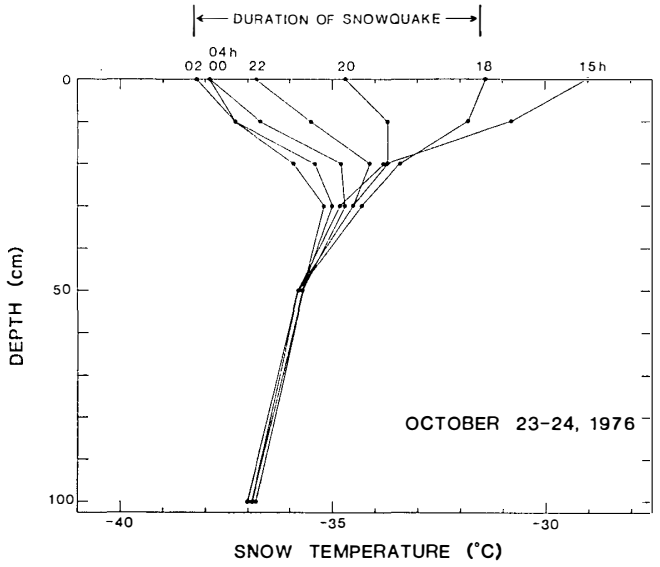

Fig. 26. Variation of snow temperature profiles during the occurrence of snowquakes on October 23–24, 1976.

temperature, and during the increase of the temperature it was completely quiet.

Figure 26 shows the variation of snow temperature profile during the occurrence of snowquake from 1800 LT October 23 to 0400 LT October 24. The change of snow temperature profiles suggests that the tensile thermal stress is induced by the decreasing snow temperature and causes the occurrence of snowquakes. The focal depth of snowquakes should be as shallow as about 50 cm since during the occurrence of snowquakes the variation of snow temperature is limited within the uppermost 50 cm of the snow cover. Furthermore, the focal depth located near the surface could be estimated by the fact that a new thermal crack, which was formed at the depth of about 20 cm, was observed just after the occurrence of snowquakes at the glazed surface as shown in Fig. 21.

5.2. Relation between strain rate and initiation of snowquakes

It was described that the snowquake activity is clearly related to the decreasing rate of snow temperature, and the snow surface temperature change at the initiation of snowquake activity seems to depend on the daily mean snow temperature. To obtain the relation between the daily mean snow surface temperature and the snow surface temperature change when snowquake begins to occur, the thermal strain rate is defined as $\alpha(\partial T/\partial t)$, where α is the linear expansion coefficient of snow given by eq. (5), T is the snow surface temperature and t is the time. Furthermore, during the decrease of the snow surface temperature, the thermal strain rate at the initiation of snowquake is calculated from $\alpha(\partial T/\partial t)$, and for the case when the snow surface temperature is falling but without the occurrence of snowquake, the maximum thermal strain rate under tension is calculated.

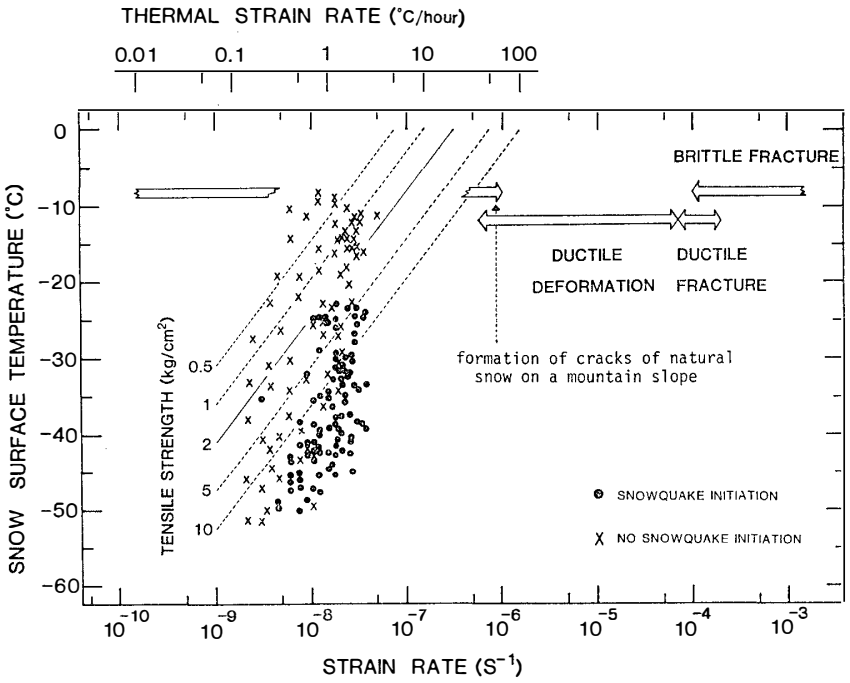

Fig. 27. Relation between the snow surface temperature and the thermal strain rate for the case of snowquake (black dots) and the case of no snowquake (crosses). Deformation behavior of snow at about −10°C is inserted after uniaxial tensile tests by NARITA *(1980).*

Figure 27 illustrates the relation between the snow surface temperature and the thermal strain rate at the initiation of snowquake activity. The black dots denote the initiation of snowquake activity, whereas the crosses indicate the maximum thermal strain rate under tension and the temperature for the cases of no snowquake activity. The black dots are located in the range of thermal strain rates of about 5×10^{-9} to $5\times10^{-8}s^{-1}$ and have a tendency to shift towards lower thermal strain rates with the decrease in the snow surface temperature at the initiation of snowquake activity. In other words, when the snow temperature was very low the snowquake takes place in small temperature change, and this leads to the thermal strain rate dependence of the fracture of the snow cover with the temperature. When snow was deformed under tensile stress, NARITA (1980) found that various deformation types were classified by different strain rates. Namely, the snow behaved as a brittle material at higher strain rates and as a ductile material at lower strain rates. As shown in Fig. 27, based upon NARITA's experiment, the transition between brittle and ductile deformations lies at a strain rate around $10^{-4}s^{-1}$ at $-10°C$ in snow temperature. The critical value of strain rate dividing the two types depends principally on snow temperature, density, texture of snow and the size of test specimens. Therefore, it is considered that the snowquake, when fracture takes place under tensile stress, is assigned to the type of ductile fracture and the snow cover behaved as a ductile material.

5.3. Amplitude and frequency of snowquakes

It is of importance to make clear the relation between the amplitude and frequency of snowquakes concerning the simultaneous observation of stress, strain, heterogeneity and their time derivatives. In this regard, considerable progress has been achieved on the implication of the amplitude–frequency relation of natural earthquake, fracture of rocks, glass and other materials, through discussion on the dependence of heterogeneity and stress condition in these materials.

The relation between the maximum trace amplitude and its frequency for natural earthquakes is expressed by the well-known Ishimoto-Iida's formula:

$$N(A)\mathrm{d}A=KA^{-m}\mathrm{d}A\ , \qquad (9)$$

where $N(A)$ is the number of earthquakes with the maximum amplitudes between A and $A+\mathrm{d}A$, and K and m are numerical constants.

The meaning of m-value in eq. (9) has been discussed by many researchers. The large m-value means relatively heterogeneous and the small one means relatively homogeneous medium (MOGI, 1962a). The m-value for volcanic earthquakes is mostly larger than 2.0 and sometimes larger than 2.0 for earthquake swarm (HAMAGUCHI and GOTO, 1978). The m-value of icequakes obtained by OMOTE *et al.* (1955), who observed ice tremors in the Lake Suwa, is 1.8 ± 0.2, and HAMAGUCHI and GOTO (1978) obtained the m-value of 1.95 ± 0.02 for the icequakes in the same lake. Thus, the m-value of 1.8 to 2.0 for icequakes almost coincides with the m-value for natural earthquakes.

On the analogy of earthquake studies, the relation between m-value and deformation of snow will be discussed to understand the physical process of fracturing of the snow cover. On the basis of amplitude–frequency distribution expressed by eq. (9),

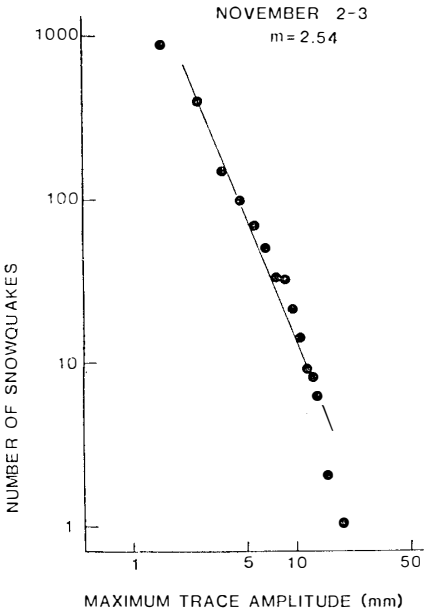

Fig. 28a. Amplitude–frequency distribution of snowquakes on November 2–3, 1976. The straight line indicates m=2.54 in the Ishimoto-Iida's formula. The interval of trace amplitude is 1 mm.

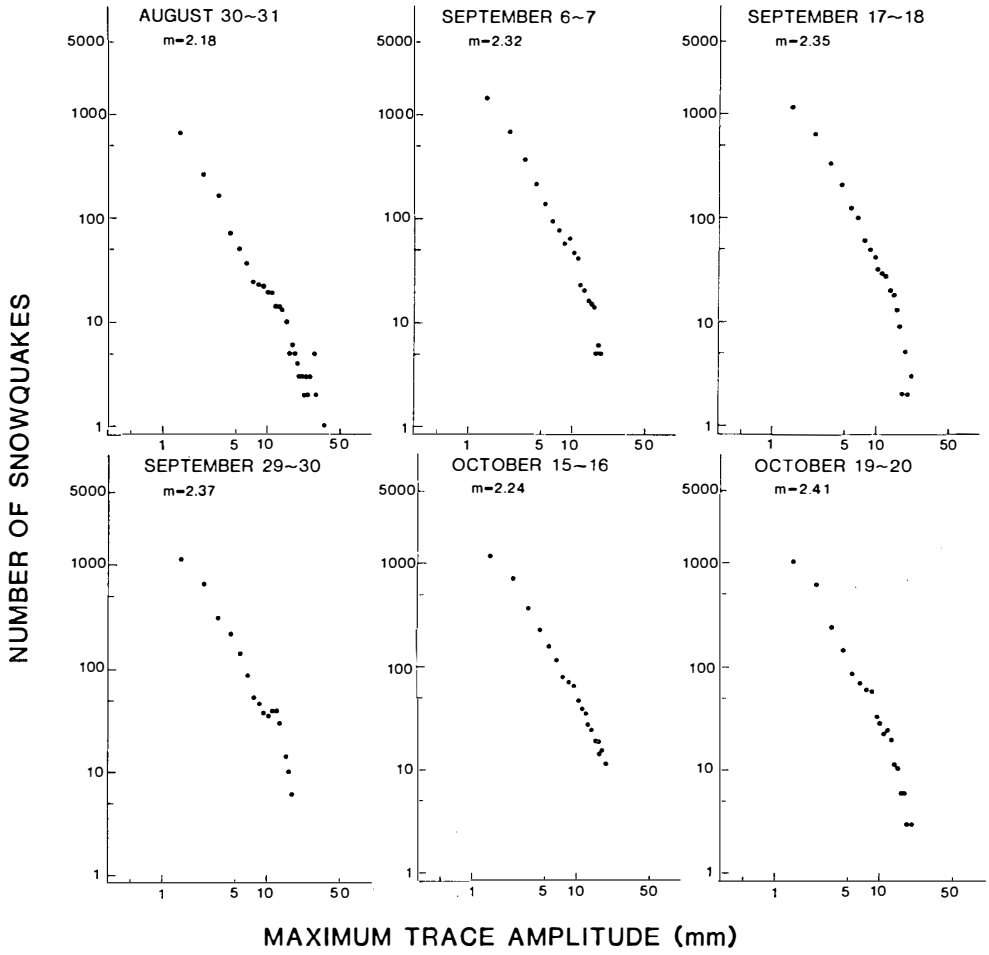

Fig. 28b. Amplitude–frequency distribution of snowquakes in 6 periods in August, September and October 1976. The m-value is also shown and the interval of trace amplitude is 1 mm.

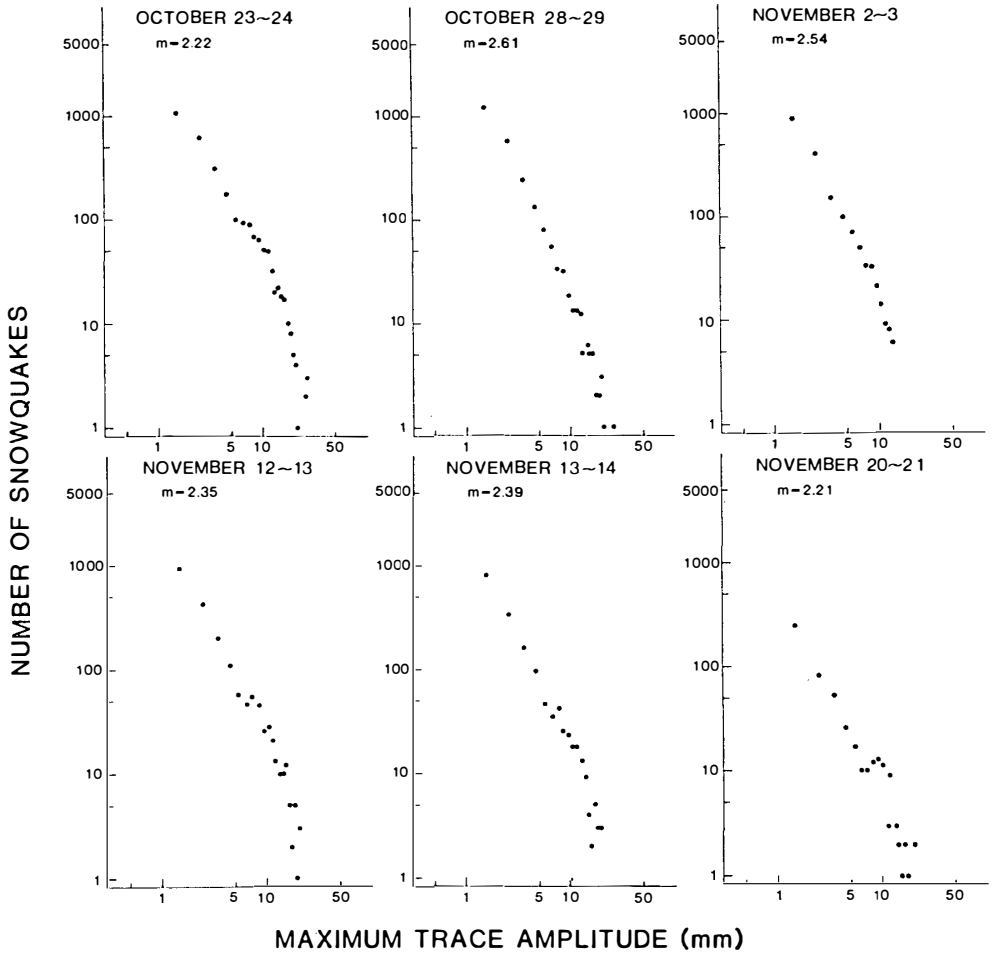

Fig. 28c. Amplitude-frequency distribution of snowquakes in 6 periods in October and November 1976. The m-value is also shown and the interval of trace amplitude is 1 mm.

the m-value for snowquakes is expressed by following UTSU (1965):

$$m=\frac{N\log e}{\sum_{i=1}^{N}\log A_i - N\log A_{\min}}+1, \tag{10}$$

where A_i is the amplitude of the i-th event, N is the number of snowquakes with the trace amplitudes larger than or equal to the smallest amplitude $A_{\min}$ which is 2.0 mm in the present study. The m-values obtained by eq. (10) for 12 cases of snowquake activity are shown in Figs. 28a, 28b and 28c. The amplitude-frequency distribution is plotted on a diagram in full logarithmic scale. As is shown in Fig. 28a, every amplitude-frequency distribution can be approximated by a straight line on the full logarithmic-scale diagram. So that the magnitude distribution of the fracturing as snowquakes generated in the thermally strained snow cover also satisfies the Ishimoto-Iida's equation for the earthquakes.

Next, the temporal variations in m-value and strain will be discussed. Figure 29 shows the relation between the m-value and the thermal strain obtained by $\alpha\cdot\Delta T$, where α is the linear expansion coefficient of snow given by eq. (5) and ΔT the dif-

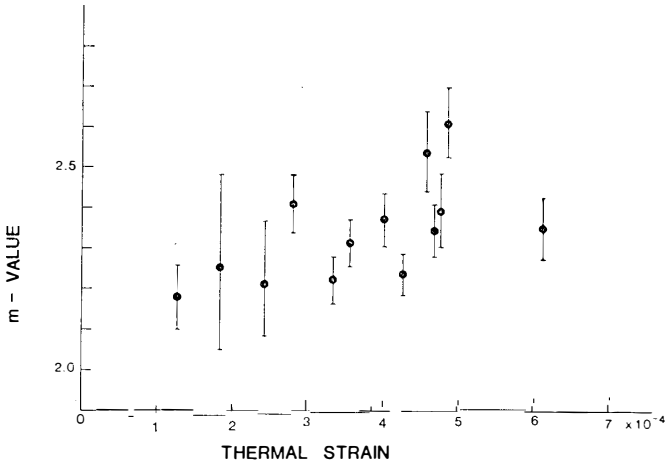

Fig. 29. The relation between m-values and thermal strain for the 13 cases between August 30 and November 22, 1976. Error bars indicate the range with 95% confidence limit.

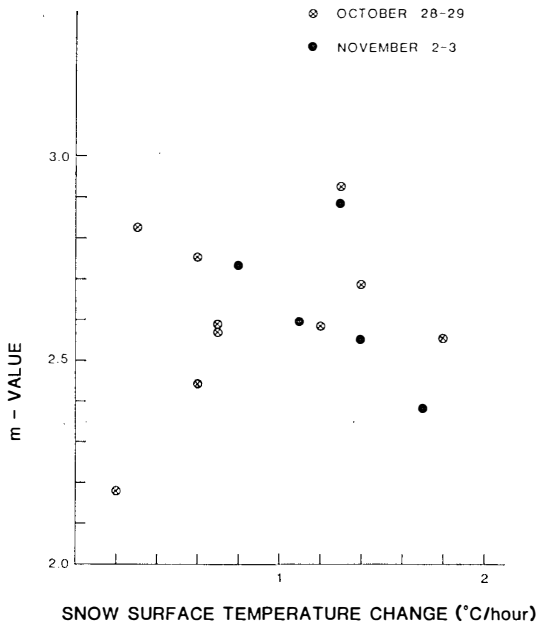

Fig. 30. The relation between m-values and snow surface temperature change (°C/hour) for snowquake swarms on October 28–29 (open circle with cross) and November 2–3 (solid circle).

ference of the snow surface temperature between the onset and the end of snowquakes during the observation period. Error bars on the solid circle are the ranges with confidence limit of 95%. The solid circle at the left end of Fig. 29 is the *m*-value for August 30–31 (see also Fig. 28b), being 2.18 ± 0.08, and the *m*-values gradually increased with the increase of thermal strain, attaining the maximum value of 2.61 ± 0.09 on October 28–29. It may be safely concluded that the *m*-value of snowquakes increases with the increase in the thermally induced strain of the snow cover.

Figure 30 shows the plotting of *m*-values against the thermal strain rate conveniently given by the snow surface temperature change (°C/hour) on October 28–29 and November 2–3. The change in *m*-value on November 2–3 is inversely proportional to the thermal strain rate (snow surface temperature change). The variation of *m*-value on October 28–29 is similar to that on November 2–3, although the *m*-values

are scattering when the strain rate is smaller than about 0.7°C/hour. The change in m-value for snowquakes is similarly found for icequakes in the Lake Suwa (HAMAGUCHI and GOTO, 1978); they suggested that the smaller m-value recognized before the large slip rate of the ice plate across the fault corresponds to the higher stress state in ice plate and that the large m-value is due to the stress relaxation.

MOGI (1962b) found that when the fracturing occurs successively in a limited region, the m-value increases gradually by an increase of the crack density with time. This suggests that the increasing in the thermal strain of snow could cause the increase of crack density and, therefore, the m-value is gradually increasing with the larger thermal strain. The m-values obtained for snowquakes are 2.18 ± 0.08 for the minimum and 2.61 ± 0.09 for the maximum. These values for snowquakes are larger than the m-value of 1.95 ± 0.02 for icequakes observed at the Lake Suwa and also larger than the common value for natural earthquakes. As was indicated by MOGI (1962a), the large m-value means relatively heterogeneous medium, apparently, the snow cover for snowquakes is a heterogeneous material in comparison with the ice plate for icequakes. The increase of m-value with the increasing thermal strain can be attributed to the increase of crack density. The m-value also depends upon the thermal strain rate as deformation in the snow cover.

5.4. Epicenter of snowquakes

As was mentioned previously, snowquakes occur when the snow temperature is decreasing and the thermal strain rate under tensile stress exceeds a critical value which becomes smaller with decreasing snow temperature. It was also mentioned that the focal depth of snowquake events should be shallow in the snow cover, accompanied with the formation of thermal cracks very near the surfae.

To determine the epicenter of each snowquake, it is assumed that the epicenter is located on the snow surface, and the location of each snowquake event is determined by an iterative least-square procedure from the arrival times of P waves in the traces of snowquake events on the recording chart. As was stated in Section 2, the accuracy of epicenter is confirmed by comparing the calculated position of artificial shots on the snow surface from the arrival times of P waves with the position of artificial shots. Thus the epicenters of artificial shots within the seismograph are usually uncertain by about ±10 m, and outside of the array uncertainties are of the order of ±10 m.

Assuming that the accuracy of epicenter of snowquakes is the order of ±10 m, the epicenters were determined from the arrival times of P waves which were clearly recorded more than 100 traces. From these traces, 38 epicenters were determined and shown in Fig. 31. These snowquakes occurred from 1847 LT to 2103 LT October 28, 1976. Figure 31 also shows the pattern of thermal cracks on the glazed surface within the seismograph array. The numerals of epicenter location indicate the time sequence of occurrence. The epicenters are located within the array and, in particular, in the area of depicted thermal cracks. This is a clear evidence that the fracture of existing thermal cracks or the formation of new thermal crack can cause the snowquake events though the accuracy of epicenter is in the order of ±10 m. Densely populated epicenters in the thermal crack area suggest the occurrence of snow-

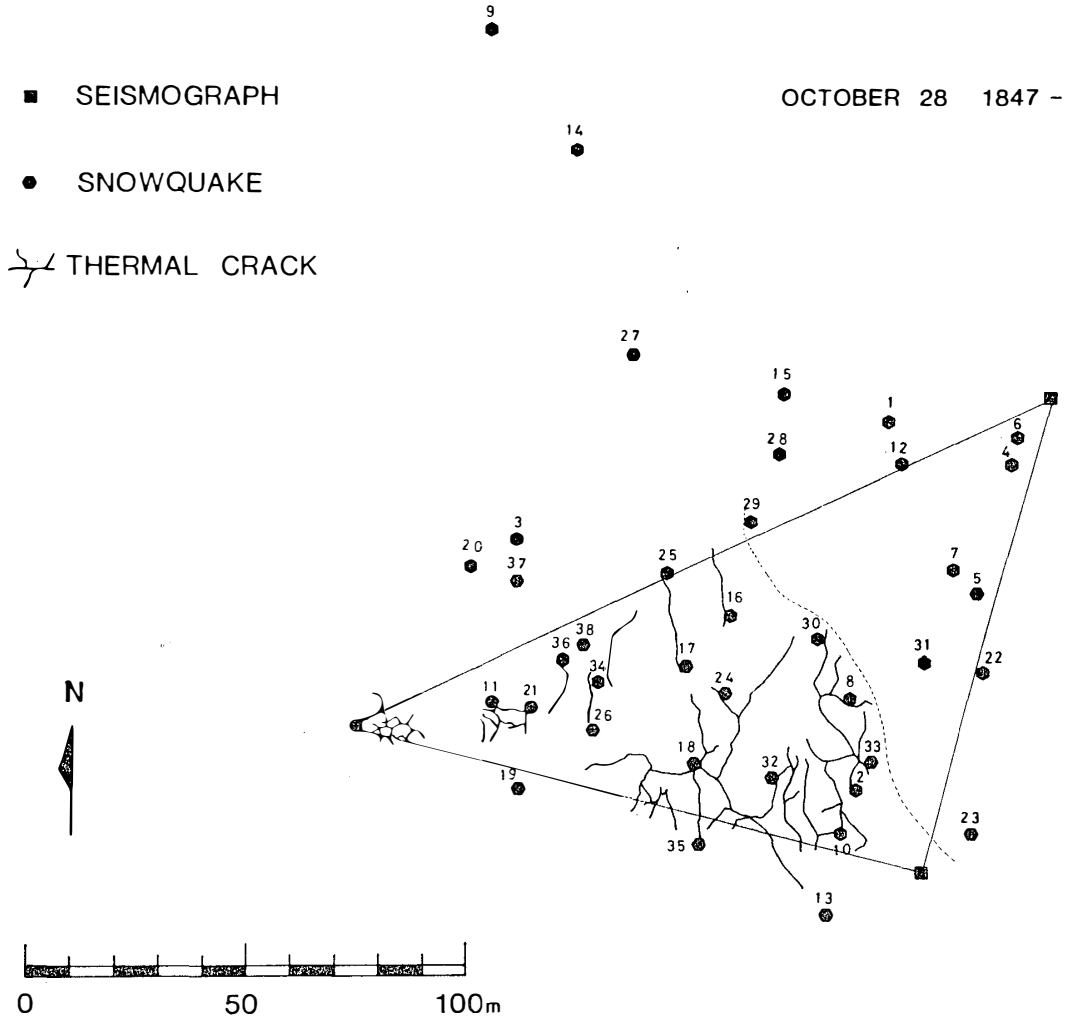

Fig. 31. Locations of epicenters of snowquakes swarms on October 28, 1976 and pattern of thermal cracks on the glazed surface within the array of seismographs. The numerals are in sequence of occurrence.

quakes at the tip of thermal crack. The numerals at each epicenter are randomly distributed. This suggests that there is no apparent correlation between snowquake activity and ordered sequence of fracturing of the snow cover.

6. Relation between Fractures and Snowquakes

Thermally induced fracture of the snow cover yields the formation of new cracks in the snow cover surface or the propagation of a crack tip from the opening of existing thermal crack. In the present section, to understand properly the process of snow fracture associated with snowquake activity, mechanical behaviors of snow are to be investigated.

6.1. Viscosity of snow

In Fig. 27 the deformation behavior during the formation of thermal cracks and snowquake activity is classified as a mode of ductile fracture in the range of strain rate from 5×10^{-9} to $5\times10^{-8}\,s^{-1}$. Hence, it is necessary to know a viscosity coefficient. To obtain the compactive viscosity coefficient η of the snow cover with the density of about 0.40 g/cm^3, the variation of thickness of a snow layer at a depth of 4 m was observed in a trench. A square about 35 cm in size was marked on the trench wall and individual side (snow layer thickness) was measured about every half a month through about half a year by using a vernier calliper. Figure 32 shows the decrease of the thickness ($\overline{BC}$ and $\overline{AD}$) of the snow layer which became thin with rising snow temperature. Compactive viscosity coefficients were calculated from both the upper

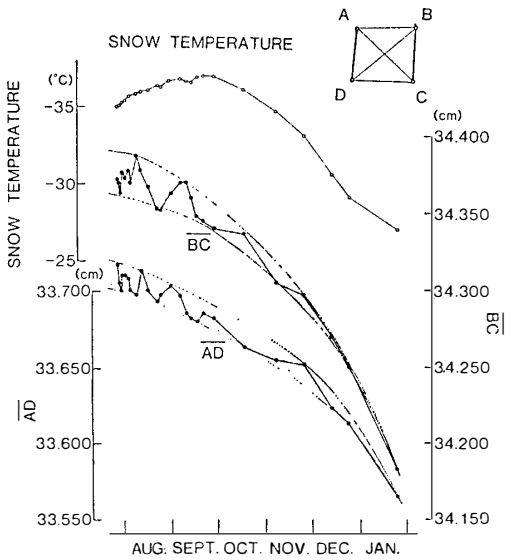

Fig. 32. Variation of the thickness of snow layer ($\overline{BC}$ and $\overline{AD}$) in the trench wall at a depth of 4 m.

and lower envelopes of the measured value of thickness corresponding to sides $\overline{BC}$ and $\overline{AD}$ of the square.

On the basis of Sorge's law of densification of snow (BADER, 1953) the compactive viscosity coefficient will be derived. The thickness of a snow layer at time t is denoted by $H(t)$, then the increment ds of strain of snow layer during a time interval dt is given by $ds=\{H(t)-H(t+dt)\}/H(t)$, and the coefficient of viscosity $\eta(t)$ of the snow composing the layer is defined by the relation $(ds/dt)_t=p(t)/\eta(t)$, where $p(t)$ is the load applied on the snow layer.

From the compaction of snow layer as shown in Fig. 32, the compactive viscosity coefficients can be calculated. If the compactive viscosity coefficients do not depend on the snow temperature, the curves shown in Fig. 32 should exhibit a simple relationship between the strain of snow layer and the time. But the thickness of snow layer is proportionally decreasing with increasing snow temperature. This fact suggests that the thinning of snow layer is mainly dependent upon the increase of snow temperature rather than the increase of snow density. From the upper and lower envelops of the snow layer $\overline{BC}$ and $\overline{AD}$ in Fig. 32, compactive viscosity coefficients were calculated. In Fig. 33 the calculated compactive viscosity coefficients are plotted against the snow temperature in the range from -25 to -40°C. The relation between the compactive viscosity coefficient and the snow temperature is obtained by averaging the upper and lower limits of the calculated values as shown in Fig. 33.

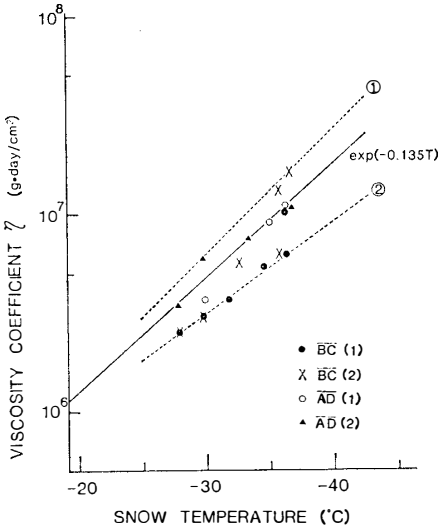

Fig. 33. Relation between snow temperature and compactive viscosity coefficient. The solid line shows $\eta=\eta_0 \exp(-0.135T)$ *obtained by the average values of the upper and lower limits (1) and (2). The solid circles and crosses indicate respectively the calculated viscosity from the upper and lower envelopes of thickness change of* $\overline{BC}$ *in Fig. 32. The open circles and solid triangles indicate respectively the calculated viscosity from the upper and lower envelopes of thickness change of* $\overline{AB}$ *in Fig. 32.*

The relationship between the snow temperature and the compactive viscosity coefficient is represented by

$$\eta=\eta_0 \exp(-0.135T), \tag{11}$$

where $\eta_0(7.05\times10^{12}\ \text{dyne}\cdot\text{s}\cdot\text{cm}^{-2})$ is the compactive viscosity coefficient at 0°C and T the snow temperature. This results is similar to the relationship of $\eta=\eta_0 \exp(-0.15T)$ given by KOJIMA (1959).

6.2. Snowquake initiation and tensile strength of snow

It was shown that the thermally induced strain rate at the initiation of snowquake is in the range of 5×10^{-9} to 5×10^{-8} s^{-1} and the initiation of snowquake is strongly dependent on the snow surface temperature. Furthermore, it was pointed out that the snow behaves as a mode of ductile fracture in the range of this thermal strain rate during snowquake activity.

We assume that the behavior in the deformation period is represented by a simple rheological model, *i.e.*, the Maxwell model.

$$\dot{\sigma}=E\dot{\varepsilon}-\frac{E}{\eta}\sigma\ ,$$

where σ is the stress which is the resisting force per unit area, $\dot{\sigma}$ the stress rate, $\dot{\varepsilon}$ the strain rate, E the Young's modulus and η the viscosity coefficient. When $\dot{\varepsilon}$ is constant and $\sigma=0$ at $t=0$, the above equation is integrated:

$$\sigma=E\tau\dot{\varepsilon}\left\{1-\exp\left(-\frac{t}{\tau}\right)\right\}\ , \tag{12}$$

where $\tau(=\eta/E)$ is the relaxation time.

Since the ductile fracture according to the thermal strain rate is considered during the snowquake activity and the relaxation time is as short as about several minutes, in the case of $(t\gg\tau)$ eq. (12) is represented by

$$\sigma=E\tau\dot{\varepsilon}\quad\text{or}\quad\eta\dot{\varepsilon}, \tag{13}$$

which will be applied to the criterion of the initiation of snowquake activity.

It is also assumed that when the thermally induced stress obtained by eq. (13) becomes larger than the tensile strength of snow, the initiation of snowquake activity could occur, that is

$$\eta\dot{\varepsilon}\geq\sigma^*\ , \tag{14}$$

where $\dot{\varepsilon}$ is the thermal strain rate given by eq. (5), η the viscosity coefficient given by eq. (11) and σ^* the tensile strength of snow.

By eq. (14), the criterion of the initiation of snowquake activity should be given by the following linear relationship between log of the thermal strain rate and the snow surface temperature:

$$T=\frac{1}{a}\ln\dot{\varepsilon}-\frac{1}{a}\ln\frac{\sigma^*}{\eta_0}\ , \tag{15}$$

where a is constant (-0.135) and η_0 the compactive viscosity coefficient at 0°C given by eq. (11). Equation (15) was introduced to discuss the criterion for the occurrence of snowquake activity in terms of snow temperature and thermal strain rate (Fig. 34).

In Fig. 34 eq. (15) is presented with thin broken lines as parameters of tensile strength of 0.5, 1, 2, 5 and 10 kg/cm^2, which indicating the case that the tensile strength is independent of snow surface temperature. However, the thick broken

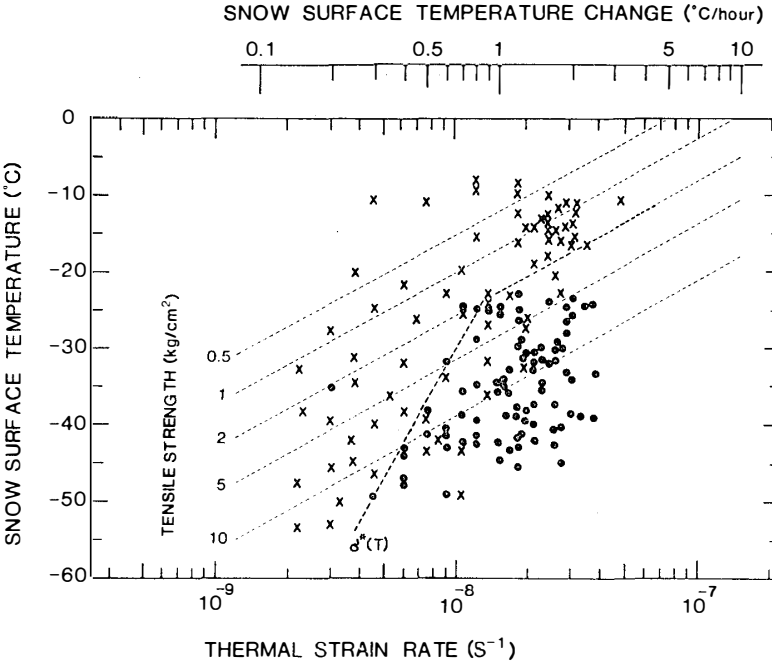

Fig. 34. Relation between the snow surface temperature and the thermal strain rate for the case of snowquake (solid circles) and no snowquakes (crosses). The thin broken lines indicate parameters of critical tensile strength of snow by eq. (15) without temperature dependence. The thick broken line is the boundary of snowquake occurrence, which suggests the temperature dependence of tensile strength of snow.

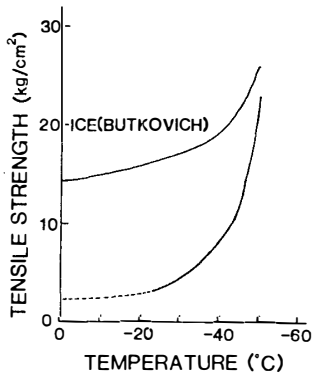

Fig. 35. Dependence of tensile strength of snow ($\rho = 0.40$) and ice (BUTKOVICH, 1954) upon temperature.

line at the threshold of the snowquake initiation suggests the temperature dependence of tensile strength of snow. It is to be remarked that the snowquakes are occurring when the snow surface temperature is below −20°C.

Figure 35 shows the temperature dependence of the tensile strength of snow obtained by the thick broken line in Fig. 34, and also the tensile strength of ice obtained by BUTKOVICH (1954). In the snow temperature range between −2.5 and −18°C around the strain rate of 10^{-6} to 10^{-5} s^{-1}, the tensile strength of snow with the density of 0.37 g/cm³ is dependent upon the snow temperature when the stress is in the range of about 0.5 bars to 1 bar (NARITA, private communication). In the present case, the tensile strength of snow is remarkably depending on the snow temperature below −20°C. Thus, the snowquake activity is initiated in a range of low snow surface temperature which gives rise to the change in strength of snow.

6.3. Thermal stress by the change of snow temperature

An elastic model is to be applied to calculate the thermal stresses in the surface snow cover for the first approximation, though the snow and ice respond elastically only over a time scale of 5 to 10 s (GOLD, 1958). For simplification, we consider a snow cover plate with the thickness in the x–z plane, the positive z direction being into the snow cover plate. Suppose that the plate undergoes a temperature change $T(z, t)$ that depends only on the time and the distance z from the surface. TIMOSHENKO

and GOODIER (1951) gave the following solution for the thermal stress developed in the plate at time t and depth z well away from a thermal crack edge,

$$\sigma_x=\sigma_z=-BT(z,t)+\frac{B}{d}\int_0^d T(z,t)\mathrm{d}z + \frac{12(z-d/2)}{d^3}B\int_0^d T(z,t)(z-d/2)\mathrm{d}z\,, \tag{16}$$

where $B=E\alpha(1-\sigma)$, and E is Young's modulus, σ the Poisson's ratio and α the linear expansion coefficient given by eq. (5). The first term of the right-hand side is the thermal stress that would be present if the temperature change $T(z,t)$ occurred in a semi-infinite medium. The second term is the adjustment due to the boundary condition of zero normal stress at the thermal crack edges of the plate of thickness d. Similarly, the third term is the adjustment due to the boundary condition of zero bending moment at the thermal crack edges.

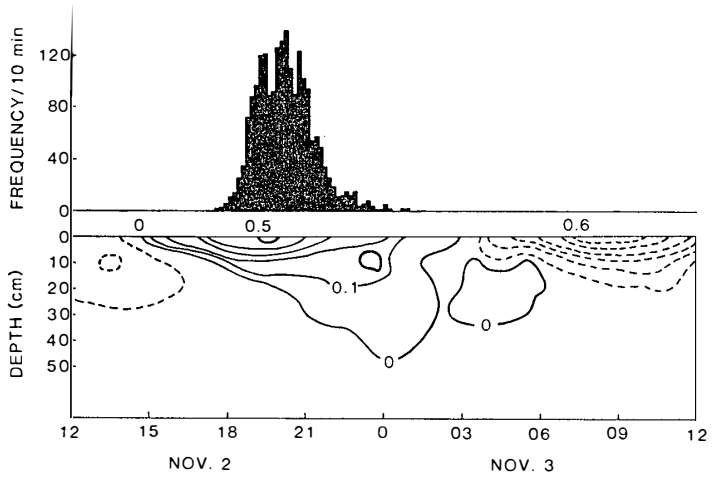

Fig. 36. Calculated distribution of thermal stress in snow (unit in bar, solid line for tension, broken line for compression) and frequency distribution of snowquakes on November 2–3, 1976.

Figure 36 shows the calculated distribution of thermal stress in the snow cover obtained by eq. (16) and the snowquakes frequency at the mean snow surface temperature of −30°C on November 2–3, 1976. The solid lines indicate the tensile stress with the maximum of 0.5 bars at the maximum snowquake activity and the broken lines gives the compressional stress with the maximum of 0.6 bar. The remarkably large tensile stress is consistent during high snowquake activity and the tensile stress to cause the fracture of snow occurs near the snow surface about 20 cm in depth. At the initiation of snowquake activity the tensile stress is about 0.4 bar which is smaller than the tensile strength of snow. The tensile strength of snow with density about 0.4 g/cm^3 at temperature of −30°C is usually around 3 bars which was obtained by many researchers. Since the stress concentration at the tip of thermal crack could occur, it is possible, therefore, that the snowquakes are initiated at a smaller tensile stress than the tensile strength of snow.

6.4. Relation between number of snowquakes and release of strain energy

Figure 37 shows the relationship between the number of snowquakes and thermal strain at the snow surface in 5-degree snow temperature range. The number of snowquakes has a good correlation with the thermal strain, namely, the number of snowquakes is linearly increasing with the increase of thermal strain. This fact indicates that the number of cracks in the snow is gradually increasing during deformation under tensile strain, consequently the snowquake events are linearly proportional to the thermal strain.

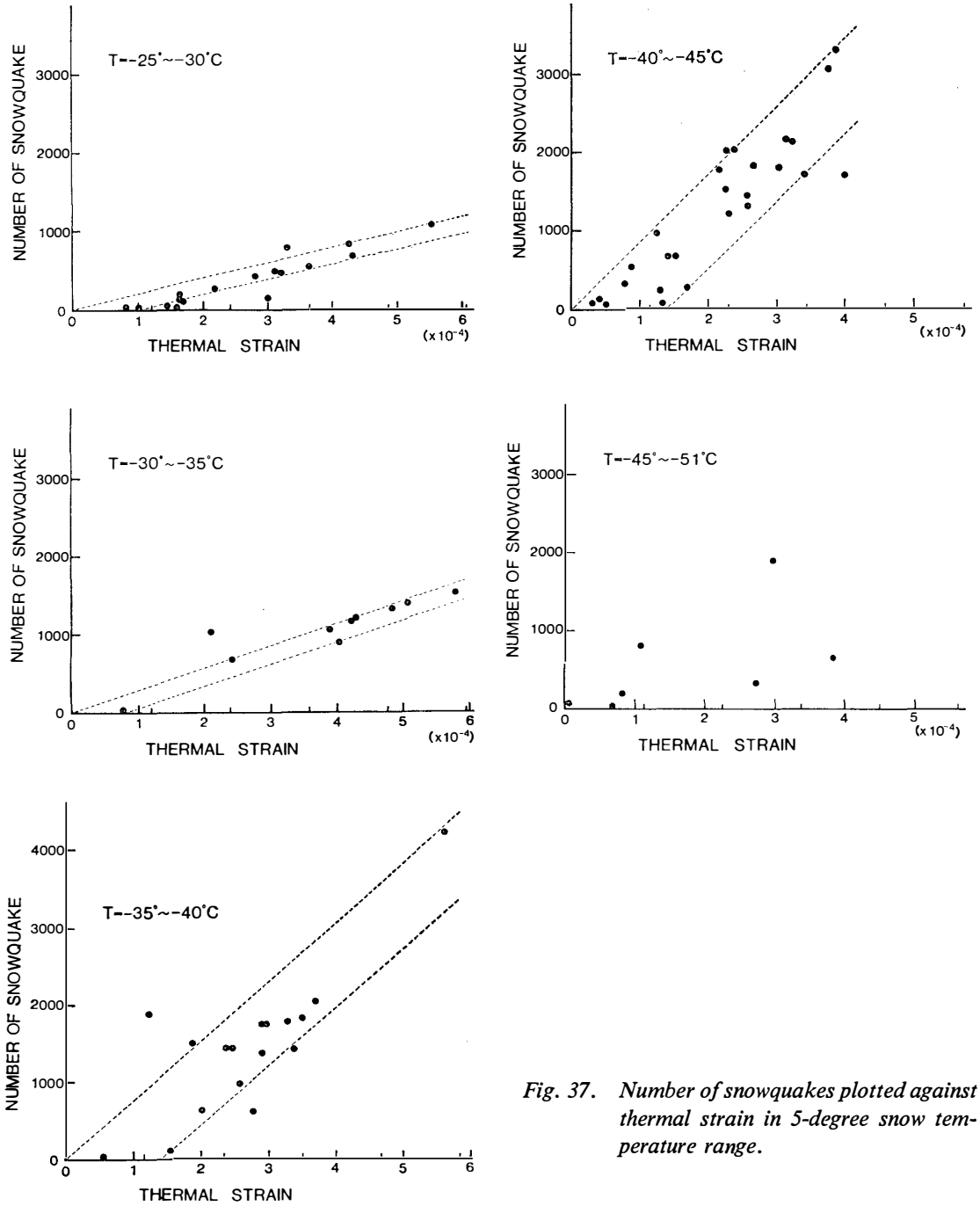

Fig. 37. Number of snowquakes plotted against thermal strain in 5-degree snow temperature range.

Furthermore, the increasing rate between the number of snowquakes and the thermal strain becomes larger with the lowering of snow temperature. At a constant strain the strain energy stored in a unit volume of snow becomes larger with the decrease of snow temperature because snow shows the strain hardening with the decrease of snow temperature. If the high strain energy of snow causes a large number of crack formation to release the strain energy, the increasing rate of the number of snowquakes becomes larger with the decrease of snow temperature.

It was found that the m-value becomes gradually larger with the increase of thermal strain. This shows that the increase of the thermal strain of snow causes the increase of the number of cracks and also the number of snowquakes. Thus, it is concluded that the number of cracks becomes large with the increase of thermal strain and the number of snowquakes increases.

7. Conclusions

To investigate the physical processes of fracture of the snow and snowquake activity, studies were carried out at Mizuho Station, East Antarctica. Studied subjects were snow temperature profiles in association with the formation of thermal crack and snowquake, distribution of the glazed surface and variation of width of thermal crack, snowquake activity, and mechanical properties of snow cover in relation to thermally induced fractures.

The results of the present study are summarized as follows:

1) The variation of snow temperature showed remarkable annual cycle and significant short periods of 7.3, 3.0 and 1.0 day, some of which were the result of the influence of cyclones penetrating into the inland during the winter and the diurnal cycle during the summer.

2) Pattern of thermal cracks on glazed surface is maintained and cracking is well propagating in response to thermal straining due to snow temperature fluctuations. However, once thermal cracks are covered with thick snow layer, the formation of cracks is unlikely unless the thermal stresses attain considerably large value to initiate cracks.

3) Variation of width of thermal cracks is explained with the thermal expansion and contraction induced by temperature waves, and the formation and growth of thermal cracks are strongly associated with snowquake activity.

4) Thermally induced fracture of the snow cover, which gave the formation of narrow cracks, was observed and the stress concentration at the tip of thermal crack causes snowquakes. The principal axis of strain in tension during the occurrence of snowquake swarm indicates the direction perpendicular to the strike of thermal crack. Therefore, the tensile stress due to thermal contraction causes formation of thermal crack and the tensile cracking takes place at the tip of thermal crack.

5) Snowquake activity is classified in three seasonal periods: during midwinter from June to August, the occurrence of snowquakes is irregular; during the spring from September to October and at the beginning of the summer in November, the snowquake activity was pronounced daily between the early evening and the early morning through midnight; and at the beginning of the summer in the end of November no snowquakes occur.

6) Fracture of snow cover under tensile stress, which causes snowquake activity, is interpreted as the type of ductile fracture.

7) The relationship between amplitude and frequency of snowquakes is expressed

by the Ishimoto-Iida's formula in seismology and the m-value of the formula is estimated to be from 2.18 to 2.61. The obtained m-values are larger than the m-value of 1.95 for icequakes observed at the Lake Suwa and also larger than the common value for natural earthquakes. Furthermore, the m-value becomes gradually larger with the increasing thermal strain which is due to the increase of crack density in the snow cover.

8) Individual snowquake event is closely associated with the formation of crack which is existing in the uppermost 50 cm of the snow cover, and the epicenters of snowquake events are located near the existing thermal cracks. Well-ordered sequential occurrence of epicenters was not observed, thus the fracturing of snow cover as cracking occurred randomly near the surface.

9) When the snow temperature is below about $-20°C$ the tensile strength of snow cover is remarkably dependent on temperature, and the snowquake activity is limited in the low temperature range which affects the increase in tensile strength of snow.

10) Since the number of cracks in the snow is increasing during deformation under tensile strain, snowquake events caused by the formation of cracks is proportional to the increasing thermal strain.

Acknowledgments

The author would like to express his thanks to Drs. T. ISHIDA, G. WAKAHAMA and N. MAENO of the Institute of Low Temperature Science, Hokkaido University, for their helpful discussions and for critically reading the manuscript. He is also grateful to Drs. K. KUSUNOKI and S. MAE of the National Institute of Polar Research, for their critical reading of this manuscript and encouragement throughout the study. He is also indebted to members of the wintering party of 17th Japanese Antarctic Research Expedition led by Prof. T. YOSHINO for generous support in the field. He wishes to express his thanks to Ms. Y. MORINAGA and Mrs. Y. UEMATSU for their assistance in preparing the manuscript.

References

BADER, H. (1953): Sorge's law of densification of snow on high polar glaciers. SIPRE Res. Rep., **2**, 3 p.

BUTKOVICH, T. R. (1954): Ultimate strength of ice. SIPRE Res. Rep., **11**, 12 p.

CARSLAW, H. S. and JAEGER, J. C. (1959): Conduction of heat in solids. 2nd ed. Oxford, Clarendon, 510 p.

FUJIWARA, K. and ENDO, Y. (1971): Preliminary report of glaciological studies. Mem. Natl Inst. Polar Res., Spec. Issue, **2**, 68–109.

GOLD, L. W. (1958): Some observations on the dependence of strain on stress for ice. Can. J. Phys., **36** (10), 1265–1275.

HAMAGUCHI, H. and GOTO, K. (1978): A study on ice faulting and icequake activity in the Lake Suwa, (2) Temporal variation of m-value. Sci. Rep. Tohoku Univ., Ser. 5 (Geophys.), **25** (1), 25–38.

HAMAGUCHI, H., SUZUKI, Z., KOYAMA, J. and GOTO, K. (1977): A study on ice faulting and icequake activity in the Lake Suwa, (1) Preliminary field observations. Sci. Rep. Tohoku Univ., Ser. 5 (Geophys.), **24** (1/2), 43–55.

ISHIZAWA, K. (1981): The measurement of the velocities of *P* and *S* waves propagating in the surface layer of ice sheet at Mizuho Station, East Antarctica. Nankyoku Shiryô (Antarct. Rec.), **73**, 147–160.

IWABUCHI, M., FUJII, R. and UTSUMI, T. (1978): Gurafikku disupurei o mochiita supekutoru kaiseki shisutemu (Conversational system of spectrum analysis by the use of graphic display). Nankyoku Shiryô (Antarct. Rec.), **62**, 29–70.

JAEGER, J. C. (1969): Elasticity, Fracture and Flow; with Engineering and Geological Applications. 3rd ed. London, Methuen, 268 p.

KAMINUMA, K. and TAKAHASHI, M. (1975): Iceshock swarms observed at Mizuho Camp, Antarctica. Nankyoku Shiryô (Antarct. Rec.), **54**, 75–83.

KOJIMA, K. (1959): Sekisetsu-sô no asshuku nensei-ritsu oyobi shôgeki hakai teikô ni oyobosu sekisetsu ondo kôbai no eikyô (The influence of temperature gradient upon the grain texture, settling rate and brittleness of snow). Teion Kagaku, Butsuri-hen (Low Temp. Sci., Ser. A, Phys.), **18**, 29–45.

LOEWE, F. (1969): On the coreless winter of the polar regions. Gerlands Beitr. Geophys., **78** (6), 453–476.

MOGI, K. (1962a): Study of elastic shocks caused by the fracture of heterogeneous materials and its relations to earthquake phenomena. Bull. Earthq. Res. Inst., **40**, 125–173.

MOGI, K. (1962b): Magnitude-frequency relation for elastic shocks accompanying fractures of various materials and some related problems in earthquakes. Bull. Earthq. Res. Inst., **40**, 831–835.

NARITA, H. (1980): Mechanical behaviour and structure of snow under uniaxial tensile stress. J. Glaciol., **26** (94), 275–282.

NARITA, H., MAENO, N. and NAKAWO, M. (1978): Structural characteristics of firn and ice cores drilled at Mizuho Station, East Antarctica. Mem. Natl Inst. Polar Res., Spec. Issue, **10**, 48–61.

NEAVE, K. G. and SAVAGE, J. C. (1970): Icequakes on the Athabasca Glacier. J. Geophys. Res., **75**, 1351–1362.

NISHIO, F. (1978): Snow temperature at Mizuho Camp in 1976–1977. JARE Data Rep., **44** (Glaciol.), 41–98.

OMOTE, S., YAMAZAKI, Y., KOBAYASHI, N. and MURAUCHI, S. (1955): Ice tremors generated in the floating lake ice (Part I). Bull. Earthq. Res. Inst., **33**, 663–679.

PATERSON, W. S. B. (1969): The Physics of Glaciers. Oxford, Pergamon, 250 p.

SANDERSON, T. J. O. (1978): Thermal stresses near the surface of a glacier. J. Glaciol., **20** (83), 257–283.

SWITHINBANK, C. W. M. (1957): The morphology of the ice shelves of western Dronning Maud Land. Norw.-Br.-Swed. Antarct. Exped., 1949–52, Sci. Res., **3**, IA (Glaciol.), 1–37.

TIMOSHENKO, S. and GOODIER, J. N. (1951): Theory of Elasticity. New York, McGraw-Hill, 506 p.

UTSU, T. (1965): Jishin no kibo-betsu dosû no tôkei-shiki $\log n = a - bM$ no keisû b o motomeru ichihôhô (A method for determining the value of b in a formula $\log n = a - bM$ showing the magnitude–frequency relation for earthquakes). Geophys. Bull. Hokkaido Univ., **13**, 99–103.

WATANABE, O. (1978): Distribution of surface features of snow cover in Mizuho Plateau, East Antarctica, 1969–1975. Mem. Natl Inst. Polar. Res., Spec. Issue, **7**, 44–62.

WATANABE, O. and YOSHIMURA, A. (1972): Mizuho Kansokukyoten fukin no seppyôgaku-teki jôtai ni tsuite (Glaciological observations in the vicinity of Mizuho Camp, Enderby Land, East Antarctica). Nankyoku Shiryô (Antarct. Rec.), **45**, 20–32.

YAMADA, T. (1975): Thermal cracks in snow cover at Mizuho Camp in 1971. JARE Data Rep., **27** (Glaciol.), 177.

YAMAJI, K. (1957): 0°–100°C no han'i no kôri no netsu bôchô (The thermal expansion of ice in the temperature range 0°–100°C). Teion Kagaku, Butsuri-hen (Low Temp. Sci., Ser. A, Phys.), **16**, 73–77.

(Manuscript received November 17, 1982;
Revised manuscript received December 15, 1982)